Title

Functional characterization of helminth-associated Clostridia reveals covariates of Treg differentiation

Authors

Shushan Sargsian[1], Alannah Lejeune[1], Defne Ercelen[2], Wen-Bing Jin[3], Alan Varghese[4], P'ng Loke[5], Yvonne A. L. Lim[6], Chun-Jun Guo[3], Ken Cadwell[7,8,9,10,*]

[1]Department of Microbiology, New York University Grossman School of Medicine, New York, NY 10016, USA

[2]Division of Gastroenterology and Hepatology, Department of Medicine, New York University Langone Health, New York, NY 10016, USA

[3]Jill Roberts Institute for Research in Inflammatory Bowel Disease, Weill Cornell Medicine, Cornell University, New York, NY 10021, USA

[4]Department of Cell Biology, New York University Grossman School of Medicine, New York, NY 10016, USA

[5]Laboratory of Parasitic Diseases, National Institute of Allergy and Infectious Diseases, National Institutes of Health, Bethesda, MD 20892, USA

[6]Department of Parasitology, Faculty of Medicine, Universiti Malaya, 50603 Kuala Lumpur, Malaysia.

[7]Division of Gastroenterology and Hepatology, Department of Medicine, University of Pennsylvania Perelman School of Medicine, Philadelphia, PA 19104

[8]Department of Systems Pharmacology and Translational Therapeutics, University of Pennsylvania Perelman School of Medicine, Philadelphia, PA 19104

[9]Department of Pathology and Laboratory Medicine, University of Pennsylvania Perelman School of Medicine, Philadelphia, PA 19104

[10]Lead Contact

***Correspondence:** ken.cadwell@pennmedicine.upenn.edu (K.C.)

Abstract

Parasitic helminths influence the composition of the gut microbiome. However, the microbiomes of individuals living in helminth-endemic regions are understudied. The Orang Asli, an indigenous population in Malaysia with high burdens of the helminth *Trichuris trichiura*, displayed microbiotas enriched in Clostridia, a class of spore-forming obligate anaerobes previously shown to have immunogenic properties. We previously isolated novel Clostridia that were enriched in these individuals and found that a subset promoted the *Trichuris* life cycle. Here, we further characterized the functional properties of these bacteria. Enzymatic and metabolomic profiling revealed a range of activities associated with metabolism and host response. Consistent with this finding, monocolonization of mice with individual isolates identified bacteria that were potent inducers of regulatory T cell (Treg) differentiation in the colon. Comparisons between variables revealed by these studies identified enzymatic properties correlated with Treg induction and *Trichuris* egg hatching. These results provide functional insights into the microbiotas of an understudied population.

Keywords: Clostridia; helminth; *Trichuris*; microbiome; immune modulation; regulatory T cells; metabolites; bacterial enzymes

Introduction

The gut microbiota and its enzymatic byproducts impact numerous aspects of host physiology including metabolism and immunity [1-9]. The composition of the microbiota has been associated with numerous disease conditions and is heavily influenced by geography and lifestyle [10-18]. However, microbiome research is dominated by studies examining individuals in highly developed countries [19, 20]. Environmental variables absent in these populations contribute to differences in their microbiome compared with individuals residing in other regions. For instance, parasitic worms known as helminths cohabitate the gastrointestinal tract alongside bacteria and influence the diversity and composition of the microbiota [21-25]. Helminths colonize 1.5 billion people, or roughly 24% of the world population, with the highest prevalence reported in tropical and subtropical areas in Africa, Asia, and South America. [26-28]. Examining the properties of intestinal bacteria enriched in individuals from helminth-endemic regions may broaden our understanding of microbiota function.

Helminth infection can cause disease involving malnutrition, impaired growth, dysentery, intestinal obstruction, and anemia [26, 27]. The incidence of helminth infections is also negatively linked to the incidence of immune-mediated disorders on a global scale [29, 30]. The immune response generated against helminths includes the differentiation and expansion of regulatory T cells (Tregs), which suppress the development of autoimmune and inflammatory diseases [31-36]. Immune modulation by helminths can occur either by direct effects on the host immune system or indirectly through the microbiota [37-41]. For example, we and others have shown that expansion of the Clostridiales order during helminth colonization ameliorates disease in mouse models of inflammatory bowel disease and allergic asthma [41, 42]. We also found that Clostridiales were enriched in the gut microbiome of the Orang Asli, an indigenous population in rural Malaysia. Clostridiales were enriched in individuals with high burdens of the whipworm *Trichuris trichiura*, and deworming medication reduced the relative abundance of Clostridiales [42].

Clostridiales and the Clostridia class to which they belong are Gram-positive, spore-forming anaerobes that influence host physiology, such as through promoting differentiation of Tregs [5, 43, 44]. Based on the above association with helminths, we recently used a chloroform-based enrichment protocol to isolate and sequence the genomes of spore-forming bacteria from the feces of helminth-colonized Orang Asli [45]. This approach identified 13 Clostridiales species, most of which represented poorly characterized taxa. Metagenomics analysis of a large number

81 of Malaysians confirmed the association of these Clostridiales members with the Orang Asli
82 population and identified a specific association between the *Peptostreptococcaceae* family and
83 helminth colonization. Also, we found that *Peptostreptococcaceae* isolates were strong inducers
84 of *Trichuris* egg hatching, suggesting that Clostridiales enriched during helminth colonization
85 contain properties that support the helminth life cycle. However, the functional properties of these
86 bacteria remain unknown. Here, we examined the enzymatic and metabolomic activity of isolated
87 bacteria and their ability to induce Treg differentiation and identified specific enzymatic properties
88 that correlated with Treg induction and *Trichuris* egg hatching.
89
90
91 **Results**
92 **Study design**
93 We previously isolated 14 distinct bacterial taxa from *T. trichiura*-colonized Orang Asli
94 (OA1-14) and assigned genus-species designation based on whole genome sequencing (Figure
95 1) [45]. OA isolates represented six Clostridiales families: *Erysipelotrichaceae*, *Coprobacillaceae*,
96 *Clostridiaceae*, *Peptostreptococcaceae*, *Oscillospiraceae*, and *Lachnospiraceae*. One of the
97 *Lachnospiraceae* members, OA3, was a new species in the *Ruminococcus* genus based on
98 sequence identity and was designated *Ruminococcus pangsunibacterium*. OA12 was identified
99 as *Enterococcus hirae*. Although not a member of the Clostridiales order, the resistance of
100 *Enterococci* to chemical treatment likely explains how this bacterium was retained after
101 fractionation [46, 47]. Similar to the other OA isolates, OA12 was enriched in Malaysian
102 microbiomes [45] and was therefore included in subsequent experiments. OA isolates were
103 analyzed for *in vitro* enzymatic and metabolomic activity, and then screened for their capacity to
104 promote Treg differentiation *in vivo*. Finally, we performed correlation analyses to look for
105 relationships between all measured variables to identify bacterial properties related to Treg
106 differentiation or *Trichuris* hatching.
107
108 **Enzymatic profile of the OA isolates**
109 OA isolates were functionally profiled for their ability to perform 57 enzymatic reactions
110 that represent common bacterial activities including carbohydrate metabolism. Taxonomically
111 related isolates were more likely to share activities (Figure 2a-c). For instance,
112 *Peptostreptococcaceae* isolates (OA2, 6 and 8) and *Clostridium perfringens*-OA15 displayed high

113 levels of acid phosphatase, esculin hydrolysis, Naphthol-AS-BI-phosphohydrolase, and glutamic
114 acid decarboxylase activities (Figure 2a) and the ability to metabolize D-glucose (Figure 2c). The
115 *Peptostreptococcaceae* isolates, in addition to *E. hirae*-OA12, also had the highest arylamidase
116 activities, both in terms of the degree of activity and the different amino acid substrates (Figure
117 2b). As expected, the two *Clostridium innocuum* isolates OA4 and OA5 displayed similar profiles
118 for the majority of the 57 parameters, although there were a few enzymatic reactions in which
119 they diverged. For instance, *C. innocuum*-OA4 but not *C. innocuum*-OA5 showed mannose and
120 raffinose fermentation activities. *E. hirae*-OA12 and *Enterocloster* species OA11 and OA13
121 displayed the broadest capacities to metabolize carbohydrates (Figure 2c). Overall, these data
122 indicate that OA isolates possess a broad range of metabolic activities, consistent with their
123 taxonomic diversity.
124
125 **OA isolates produce short chain fatty acids and hydrogen sulfide**
126 Given the link between helminth-associated microbiota and anti-inflammatory responses,
127 we measured the production of short chain fatty acids (SCFAs) and hydrogen sulfide (H_2S) by
128 the OA isolates. Bacteria ferment soluble fibers to produce short chain fatty acids (SCFAs) which
129 include acetate, propionate, and butyrate [48]. SCFAs have been shown to regulate a variety of
130 immune cell types [9]. For example, they can induce Treg expansion in the gut to regulate
131 intestinal inflammation [49-51]. Although levels varied, we detected acetate in the culture
132 supernatant for all 14 OA isolates. *C. innocuum*-OA4 and -OA5 and *C. perfringens*-OA14
133 produced butyrate at levels similar to or greater than acetate. Propionate was not detected or
134 negligible except for *Paraclostridium sordellii*-OA8, the two *Romboutsia hominis*-OA2 and -OA6,
135 and *Enterocloster sp*. OA11 (Figure 3a). We validated this finding by testing cecal samples from
136 mice monocolonized with *R. hominis*-OA2 and included germ-free (GF) mice as a negative
137 control and mice colonized with a previously described synthetic minimal flora (MF) consisting of
138 15 bacteria [52, 53] as a positive control. As expected, we detected minimal levels of SCFAs in
139 GF mice compared with MF mice in which all three were detected. Mice monocolonized with OA2
140 displayed the proportion of the three SCFAs predicted by the *in vitro* analysis (Figure 3b).
141 Some bacteria can produce hydrogen sulfide (H_2S), which suppresses inflammation in
142 multiple disease models and is associated with Treg differentiation [54-59]. We found that
143 *Peptostreptococcaceae* isolates OA2, 6 and 8, as well as *Enterocloster* isolates OA11 and OA13,

144 were potent producers of H_2S, suggesting another possible mechanism by which these bacteria
145 could have immunomodulatory interactions with the host (Figure 3c-d).
146
147 **Several OA isolates induce regulatory T cells in the gut**
148 Peripherally induced Tregs (iTregs) in the gut that develop in response to microbial
149 antigens and metabolites are distinguished by expression of the transcription factor *forkhead box*
150 *P3* (*Foxp3*) and *RAR-related orphan receptor γt* (*Rorγt*). These Foxp3$^+$ Rorγt$^+$ Tregs contribute to
151 immune tolerance of the microbiota and suppress colitis [60-64]. iTregs can be further
152 distinguished from thymus-derived or natural Tregs (nTregs) reactive to self-antigens by the
153 absence of the transcription factor Helios (Ikzf2) [65]. GF mice possess low numbers of iTregs,
154 and thus, the induction of iTregs in GF mice in response to colonization by bacteria serves as a
155 sensitive assay to measure immunomodulatory potential of commensal species [61, 66-68].
156 We analyzed iTregs in the colonic lamina propria of GF mice by flow cytometry three to
157 four weeks post oral inoculation with individual OA isolates (Figure 4a), except *Lawsonibacter* sp.
158 OA9 which failed to colonize GF mice in the absence of other bacteria. In addition to conventional
159 specific pathogen free (SPF) mice and untreated GF mice that served as benchmarks, we
160 included several controls to aid in interpretation of the quantitative data. As a positive control, we
161 colonized mice with a mixture of 17 Clostridia isolates (KH mix) previously shown to induce Tregs
162 in GF mice [5]. As negative controls, we used mice monocolonized with segmented filamentous
163 bacteria (SFB), a bacterium that induces Th17 cells (Rorγt$^+$ Foxp3$^-$ CD4$^+$ T cells) without inducing
164 Tregs [69], and mice monocolonized with one of the KH mix strains, *Clostridium aldenense*
165 (KH28), which is insufficient to induce Tregs to levels achieved with the entire KH mix consortium
166 [5]. We also quantified Tregs in MF mice described above (mice raised in a gnotobiotic isolator
167 containing MF) and GF mice gavaged with stool from MF mice (MF stool). Stable colonization
168 was confirmed for all conditions based on detection of bacteria in stool (Figure S1A).
169 As expected, GF mice had lower frequencies of Rorγt$^+$ Helios$^-$ Tregs out of all Foxp3$^+$ cells
170 and lower Foxp3$^+$ Rorγt$^+$ Tregs out of CD4$^+$ cells compared to SPF, MF, MF stool and KH mix
171 groups (Figure 4b-c). We observed a spectrum of Treg induction by the OA isolates. The
172 proportion of Foxp3$^+$ Rorγt$^+$ Tregs and Foxp3$^+$ Rorγt$^+$ Helios$^-$ Tregs were restored to similar levels
173 as SPF or MF mice in mice monocolonized with several of the OA isolates including *P. sordellii*-
174 OA8, *E. hirae*-OA12, and *C. perfringens*-OA14. In contrast, several OA isolates such as *R.*
175 *pangsunibacterium*-OA3 and *Lawsonibacter asaccharolyticus*-OA10 were similar to SFB and

176 failed to induce significant increases in these Treg populations. Mice monocolonized with KH28
177 increased the frequency of Foxp3$^+$ Rorγt$^+$ Tregs out of CD4$^+$ cells but not Rorγt$^+$ Helios$^-$ Tregs out
178 of Foxp3$^+$ cells (Figure 4b-c). In addition to changes in the proportion of these populations, we
179 quantified the absolute number of Tregs per colon. This analysis largely confirmed the above
180 findings by showing that OA isolates that increased the relative frequency of Foxp3$^+$ Rorγt$^+$ Tregs
181 and Foxp3$^+$ Rorγt$^+$ Helios$^-$ Tregs also increased the total number of these cells (Figure S1b-c).
182
183 **Treg induction by OA isolates correlates with Th17 but not colonization levels**
184 Given their role in mucosal immunity [70, 71], we examined whether OA isolates affect
185 the proportion of Th17 cells (Rorγt$^+$ Foxp3$^-$ CD4+ T cells) (Figure 4a) in the gut. Similar to Tregs,
186 we found that monocolonization with OA isolates led to a range of Th17 cell levels in the colon,
187 although none reached the extraordinarily high levels detected in mice monocolonized with SFB
188 (Figure 5a, S1d). Excluding SFB, we found that the proportion of Th17 cells in the colon roughly
189 correlated with the proportion of Tregs (Figure 5b). There were notable exceptions, such as OA6,
190 which was a strong Treg inducer but did not increase the frequency of Th17 cells above levels
191 seen in GF mice.
192 These observations raised the possibility that T cell differentiation reflected the degree of
193 colonization by bacteria. However, there were no significant correlations between the bacterial
194 burden and the proportions of Tregs or Th17 cells (Figure 5c-e), suggesting that the level of T
195 cell differentiation is a specific property of each bacterium. Interestingly, we found that
196 colonization by some OA isolates increased total bile acids (BAs) detected in the stool compared
197 with GF mice (Figure S2). Transformation of BAs by gut bacteria is associated with differentiation
198 of Tregs and Th17 cells [72-75]. However, we did not observe a correlation between total BAs
199 and these T cell populations.
200
201 **Correlations between properties of OA isolates**
202 To identify relationships between the properties measured for each OA isolate, we
203 performed a spearman correlation analysis between all measured variables (Figure S3). This
204 analysis identified several enzymatic activities that were correlated with T cell differentiation
205 (Figure 6a). Induction of Tregs was positively correlated with alanine arylamidase and tyrosine
206 arylamidase activity by bacteria (Figure 6a-e). Th17 cell induction was also positively correlated
207 with tyrosine arylamidase activity, and additionally associated with α-chymotrypsin activity (Figure

208 6a, f-i). Alanine arylamidase and tyrosine arylamidase have not previously been linked to Treg or
209 Th17 cell biology. α-Chymotrypsin is a member of the serine protease family and has been shown
210 to have antibacterial properties [76], and is also made by pathogenic bacteria in the *Vibrio* genus
211 [77]. Whether this correlation reflects a role of α-chymotrypsin in Th17 cell induction or merely
212 reflects the pro-inflammatory capacity of bacteria that produce this protease and induce Th17
213 cells through other mechanisms remains to be determined.

214 To quantify how bacterial properties explain the variance in lymphocyte differentiation we
215 performed a distance-based redundancy analysis (dbRDA) using the characteristics found to be
216 most significantly related with Treg or Th17 induction according to the Spearman correlation
217 analysis and LASSO regression (Figure S4a-b, Table S1). The analysis revealed that these
218 variables together contribute to the variance of responses in Treg and Th17 induction, with the
219 variation in alanine arylamidase production accounting for 41.95% of the variance, and all other
220 variables accounting for less than 20% of the variance each (Figure S4c).

221 We also incorporated data from our previous study in which we quantified the ability of
222 the OA isolates to mediate hatching of eggs from *T. trichiura* and the mouse parasite *Trichuris*
223 *muris* [45]. Hatching of *T. trichiura* but not *T. muris* was positively correlated with H_2S production
224 and negatively correlated with salicin acidification by the OA isolates (Figure 7a-c). H_2S, in
225 addition to being involved in a wide variety of physiological processes, has been shown to
226 promote hatching of eggs from *Ascaris suum*, a helminth that infects pigs [78]. Salicin utilization
227 by bacteria was previously shown to be toxic to nematodes in soil [79], although these
228 experiments were not done with *Trichuris* species. Our finding that these bacterial properties are
229 significantly related to egg hatching of only the human whipworm could provide insight on
230 mechanisms that may differentiate dependencies of *T. trichiura* and *T. muris* on bacterial factors
231 for hatching. Valine arylamidase activity was significantly correlated with hatching of both *T. muris*
232 and *T. trichiura* eggs (Figure 7a, d-e). Valine arylamidases were among the proteases found to
233 be part of the excretory/secretory products of *Contracaecum rudolphii*, a nematode that infects
234 mammals and birds [80]. This observation suggests a role for this protease in *Trichuris* egg
235 hatching.
236

237 **Discussion**

238 Our comprehensive enzymatic profiling of OA isolates coupled with analysis of SCFAs
239 and H_2S production revealed a broad range of metabolic activities that are associated with host

240 physiology, including immunity. Consistent with this observation, several OA isolates increased
241 the number and proportion of colonic iTregs when introduced into GF mice, comparable to levels
242 achieved upon colonization with the mixture of 17 Clostridia strains used as our benchmark.
243 SCFAs were previously associated with the ability of the Clostridia mixture to induce Tregs [5, 6].
244 We did not observe a correlation between SCFA production and iTreg induction by the OA
245 isolates, indicating that SCFAs are not sufficient to distinguish Treg-inducing OA isolates.
246 Subsequent to the initial characterization of the Clostridia mixture, other metabolites such as bile
247 acids have been shown to mediate Treg differentiation in the presence of intestinal bacteria [81],
248 which may contribute to Treg differentiation induced by OA isolates. Alternatively, it is possible
249 that previously unknown factors are involved. For example, we identified strong positive
250 correlations between Treg induction and alanine arylamidase and tyrosine arylamidase activities
251 that warrant further study. Our observation that three different species, *R. hominis*-OA2, *P.*
252 *sordellii*-OA8, and *E. hirae*-OA12, consistently exhibited the highest Treg and Th17 cell induction
253 as well as arylamidase activity, suggests a predictive potential for these enzymes in identifying
254 bacteria with immunomodulatory capacity. Overall, this is one of the few studies that have
255 functionally profiled individual bacterial isolates from understudied populations beyond inferring
256 properties from genomic data.
257 The ability of some OA isolates to induce both Tregs and Th17 cells is consistent with the
258 co-regulation of these cell types. Thus, a model in which helminth-associated bacteria inhibit
259 inflammatory diseases by shifting the balance towards immune tolerance may be too simplistic.
260 Although our approach allowed us to examine properties of individual bacteria in isolation and
261 reduce variables, it would be interesting to determine whether the presence of *Trichuris* alters the
262 properties of OA isolates, or vice versa. Along these lines, we noted correlations between
263 *Trichuris* egg hatching as determined in our prior study, and H_2S production and valine
264 arylamidase activity. In addition, the helminth-associated *Peptostreptococcaceae* isolates *R.*
265 *hominis*-OA2, *R. hominis*-OA6, and *P. sordellii*-OA8 had high glutamic acid decarboxylase (GAD)
266 activity which is lacking in *E. hirae*-OA12, an isolate that fails to induce *T. muris* and *T. trichiura*
267 egg hatching (Figure 2A) [45]. GAD catalyzes the formation of the neurotransmitter gamma-
268 aminobutyric acid (GABA), and bacterially produced GAD and GABA have been shown to act on
269 *Caenorhabditis elegans*, a nematode related to *Trichuris* [82]. *Trichuris* species are not
270 genetically tractable. Therefore, we suggest that testing the role of bacterial products downstream

271 of the above enzymatic pathways may lead to insights into the life cycle of this medically important
272 parasite.

273 In conclusion, our findings describe the functional properties of bacteria isolated from
274 helminth-colonized individuals in Malaysia and identify correlates of Treg induction and *Trichuris*
275 egg hatching. Although our analyses focused on a finite set of parameters and bacterial taxa,
276 they unveil key features of these specific helminth-associated bacteria that can be targeted for
277 deeper analysis in future studies. As more bacteria from individuals in understudied populations
278 become available for study along with their full genomes, it will be important to determine the
279 extent to which these functional properties are represented in related taxa, which will enable us
280 to infer how the selective presence of these bacteria in certain populations can impact their health
281 status.

Acknowledgements

We would like to thank Margie Alva, Juan Carrasquillo and David Basnight for their help in the NYU Gnotobiotic Facility, the NYU Flow Cytometry Core for training and access to equipment, and the NYU Reagent Preparation service for providing bacterial media. We would also like to thank Drew Jones, P'ng Loke, Victor Torres, Juan Lafaille, and members of the Cadwell and Loke Labs for their constructive comments. Figure 1 was created using BioRender.com. This work was in part funded by NIH grants DK093668 (K.C.), HL123340 (K.C.), AI130945 (K.C., P.L., Y.A.L.L.), AI140754 (K.C.), DK124336 (K.C.), AI121244 (K.C.), AI133977 (P.L.), 1DP2HD101401-01, (C.J.G.), DK135816-01 (C.J.G.), and 2T32AI007180 (S.S.). Further funding was provided by the Faculty Scholar grant from the Howard Hughes Medical Institute (K.C.), Crohn's & Colitis Foundation (K.C.), Kenneth Rainin Foundation (K.C.), Judith & Stewart Colton Center of Autoimmunity (K.C.), SMRT Grant Competition award from Pacific Biosciences (K.C.), W.M. Keck Foundation (C.J.G.), Kenneth Rainin Foundation (C.J.G.), and RAPP funding from Weill Cornell Medicine (C.J.G.).

Author Contributions

S.S. and K.C. conceived and designed the study. S.S. performed the experiments and analyzed and interpreted the data. A.L. helped perform enzyme assays and A.V. helped perform H_2S assays. W.B.J. and C.J.G. performed and analyzed LC-MS to quantify SCFAs. D.E. performed the effect size analysis and assisted with computational and statistical analyses. K.C., P.L. and Y.A.L.L. oversaw interpretation of the data. S.S. and K.C. wrote the paper with input from all authors.

Declaration of Interests

K.C. has received research support from Pfizer, Takeda, Pacific Biosciences, Genentech, and Abbvie; consulted for or received honoraria from Vedanta, Genentech, and Abbvie; and is an inventor on U.S. patent 10,722,600 and provisional patent 62/935,035 and 63/157,225.

311 **Main figures - titles and legends**

312

313 **Figure 1. Study design for characterization of the OA isolates**

314 List of OA isolates with updated taxonomic classifications (top) and schematic summarizing the
315 study design (bottom). The phylogenetic tree to the left of the table depicts the relationships
316 between OA isolates. The column labeled "*Trichuris* associated" refers to whether the abundance
317 of the isolate decreased in microbiomes after deworming treatment, with 'N.D.' denoting isolates
318 that were not detected [45]. The column labeled "Promotes *Trichuris* life cycle" refers to whether
319 the isolate promotes *Trichuris muris* egg hatching, with gray cells denoting isolates that were not
320 tested [45].

321 * OA4 and OA5 were classified as members of the *Erysipelotrichaceae* family and OA3 was
322 classified as a member of the *Lachnospiraceae* family at the time of our previous publication [45].

323 ** OA8 was classified as *Paraclostridium sordellii* at the time of our previous publication [45].

324 SCFA, short chain fatty acids; H_2S, hydrogen sulfide; BA, bile acids.

325

326 **Figure 2. Enzymatic profile of the OA isolates**

327 Enzyme activity (A), arylamidase activity (B), and acid production from various carbohydrates (C)
328 by the OA isolates were measured using API colorimetric kits for microbial identification. Each
329 reaction was run in at least three independent trials for each isolate, and the intensity of the
330 reaction was assessed visually on a scale of 0 (no reaction) to 4 (strong or complete reaction).
331 The phylogenetic tree at the top of (A) depicts the relationships between OA isolates.

332

333 **Figure 3. OA isolates produce short chain fatty acids and hydrogen sulfide**

334 (A) Short chain fatty acid (SCFA) production in bacterial culture supernatants measured by mass
335 spectrometry. AUC, Area under curve.

336 (B) SCFA concentration per mg of cecal contents from germ-free (GF), minimal flora (MF) or *R.*
337 *hominis*-OA2-monocolonized (OA2) mice, measured by mass spectrometry. AUC, Area under
338 curve.

339 (C) Representative images of lead acetate paper used to detect hydrogen sulfide (H_2S)
340 production by the OA isolates *in vitro*. Darker color indicates more H_2S produced by bacterial
341 cultures.
342 (D) Quantification of H_2S production by each OA isolate, normalized to the amount of H_2S
343 production by media alone ('PYG') within each experiment. Kruskal-Wallis with Dunn's multiple
344 comparisons test was used to compare between each group and PYG. *$p < 0.05$, **$p < 0.01$, ***p
345 < 0.001, ****$p < 0.0001$.
346
347 **Figure 4. OA isolates induce iTregs in the colon**
348 (A) Representative flow cytometry gating strategy for Rorγt$^+$ Helios$^-$ iTregs out of Foxp3$^+$ cells,
349 Foxp3$^+$ Rorγt$^+$ iTregs out of CD4$^+$ cells, and Rorγt$^+$ Foxp3$^-$ Th17 cells out of CD4$^+$ cells from colon
350 lamina propria cells.
351 (B) Frequencies of Rorγt$^+$ Helios$^-$ cells within Foxp3$^+$ Tregs.
352 (C) Frequencies of Rorγt$^+$ Foxp3$^+$ Tregs out of CD4$^+$ T-cells.
353 SPF, Specific pathogen free; MF, Minimal flora mice; MF stool, GF mice gavaged with stool from
354 Minimal flora mice; KH mix, Mice gavaged with consortium of 17 Clostridia strains from Atarashi
355 et al., 2013 [5]; KH 28, *Clostridium aldenense* from the KH mix; SFB, Segmented filamentous
356 bacteria; GF, Germ-free. Each dot corresponds to one mouse. Each group was tested in at least
357 2 independent experiments consisting of 2-5 mice. Kruskal-Wallis with Dunn's multiple
358 comparisons test was used to compare between each group and GF. *$p < 0.05$, **$p < 0.01$, ***p
359 < 0.001, ****$p < 0.0001$.
360
361 **Figure 5. Associations between OA isolate colonization, Tregs, and Th17 cell levels**
362 (A) Frequencies of Rorγt$^+$ Foxp3$^-$ Th17 cells out of CD4$^+$ T-cells.
363 (B) Spearman correlation between the frequency of Foxp3$^+$ Rorγt$^+$ iTregs out of CD4$^+$ cells and
364 Rorγt$^+$ Foxp3$^-$ Th17 cells out of CD4$^+$ cells induced by each bacterium or control group.
365 (C-E) Spearman correlation between the bacterial burden in each mouse and the proportions of
366 Rorγt$^+$ Helios$^-$ iTregs out of Foxp3$^+$ cells (C), Foxp3$^+$ Rorγt$^+$ iTregs out of CD4$^+$ cells (D), or Rorγt$^+$
367 Foxp3$^-$ Th17 cells out of CD4$^+$ cells (E).
368
369 In A: SPF, Specific pathogen free; MF, Minimal flora mice; MF stool, GF mice gavaged with stool
370 from Minimal flora mice; KH mix, Mice gavaged with consortium of 17 Clostridia strains from

371 Atarashi et al., 2013 [5]; SFB, Segmented filamentous bacteria; GF, Germ-free. Each dot
372 corresponds to one mouse. Each group was tested in at least 2 independent experiments
373 consisting of 2-5 mice. Kruskal-Wallis with Dunn's multiple comparisons test was used to
374 compare between each group and GF. *$p < 0.05$, **$p < 0.01$, ***$p < 0.001$, ****$p < 0.0001$.
375
376 In B-E: r^2 and p values are depicted on each plot. Each dot corresponds to the average of at least
377 2 independent repeats with 2-5 mice within each experiment and the red line depicts the linear
378 regression slope.
379
380 **Figure 6. Treg and Th17 cell induction by the OA isolates is correlated with enzymatic**
381 **activities by bacteria**
382 (A) Spearman r and p values corresponding to significant correlations between the frequency of
383 induced Treg and Th17 cells and other measured variables of the OA isolates.
384 (B) Graph displaying relationship between alanine arylamidase activity and induction of Rorγt$^+$
385 Helios$^-$ Foxp3$^+$ iTregs for the OA isolates.
386 (C) Quantification of Rorγt$^+$ Helios$^-$ Foxp3$^+$ iTregs comparing OA isolates with or without alanine
387 arylamidase activity.
388 (D) Graph displaying relationship between tyrosine arylamidase activity and induction of Rorγt$^+$
389 Foxp3$^+$ Tregs for the OA isolates.
390 (E) Quantification of Rorγt$^+$ Foxp3$^+$ Tregs comparing OA isolates with or without tyrosine
391 arylamidase activity.
392 (F) Graph displaying relationship between tyrosine arylamidase activity and induction of Rorγt$^+$
393 Foxp3$^-$ Th17 cells for the OA isolates.
394 (G) Quantification of Rorγt$^+$ Foxp3$^-$ Th17 cells comparing OA isolates with or without tyrosine
395 arylamidase activity.
396 (H) Graph displaying relationship between α-chymotrypsin activity and induction of Rorγt$^+$ Foxp3$^-$
397 Th17 cells by the OA isolates.
398 (I) Quantification of Rorγt$^+$ Foxp3$^-$ Th17 cells comparing OA isolates with or without α-
399 chymotrypsin activity.
400

401 In B, D, F, H: Spearman r and p values are depicted on each plot in. Each dot corresponds to the
402 average value per OA isolate and the red line depicts the linear regression slope. Bar graphs
403 show mean +/- SEM.
404 In C, E, G, I: Each dot corresponds to the average value per OA isolate. Mann-Whitney test with
405 p values depicted on the bar graphs.
406
407 **Figure 7. H_2S, salicin acidification, and valine arylamidase are associated with *Trichuris***
408 ***egg* hatching by bacteria**
409 (A) Spearman r and p values corresponding to significant correlations between *Trichuris* egg
410 hatching and other measured variables of the OA isolates.
411 (B) Relationship between H_2S production by the OA isolates and *T. trichiura* egg hatching rate.
412 (C) Relationship between acid production from salicin by the OA isolates and *T. trichiura* egg
413 hatching rate.
414 (D) Relationship between valine arylamidase activity by the OA isolates and *T. trichiura* egg
415 hatching rate.
416 (E) Relationship between valine arylamidase activity by the OA isolates and *T. muris* egg hatching
417 rate.
418 Spearman r and p values are depicted on each plot. Each dot corresponds to the average value
419 per OA isolate and the red line depicts the linear regression slope.

420 **Supplemental figures - titles and legends**

421

422 **Figure S1. Bacterial burden and absolute numbers of Treg and Th17 cells induced by the**
423 **OA isolates**

424 (A) Colony forming units (CFUs) per mg of stool from mice colonized with indicated bacteria on
425 the day cells were collected for analysis by flow cytometry. Each dot corresponds to one mouse.
426 (B-D) Absolute numbers of Rorγt$^+$ Helios$^-$ Foxp3$^+$ Tregs (B), Rorγt$^+$ Foxp3$^+$ Tregs (C) and Rorγt$^+$
427 Foxp3$^-$ Th17 cells (D) in the colon lamina propria of mice colonized with the indicated bacteria.

428

429 SPF, Specific pathogen free; MF, Minimal flora mice; MF stool, GF mice gavaged with stool from
430 Minimal flora mice; KH mix, Mice gavaged with consortium of 17 Clostridia strains from Atarashi
431 et al., 2013; SFB, Segmented filamentous bacteria; GF, Germ-free. Each dot corresponds to one
432 mouse. Each group was tested in at least 2 independent experiments consisting of 2-5 mice.
433 Kruskal-Wallis with Dunn's multiple comparisons test was used to compare between each group
434 and GF in B-D. *$p < 0.05$, **$p < 0.01$, ***$p < 0.001$, ****$p < 0.0001$.

435

436 **Figure S2. Monocolonization with a subset of OA isolates increases total bile acids in stool**

437 Quantification of total bile acids per g of stool from mice monocolonized with the indicated
438 bacteria. PBS, PBS as a technical control; GF, germ-free mouse; MF, minimal flora mouse.
439 Kruskal-Wallis with Dunn's multiple comparisons test was used to compare between each group
440 and GF. **$p < 0.01$, ****$p < 0.0001$.

441

442 **Figure S3. Spearman correlation matrix depicting relationships between OA isolate**
443 **properties**

444 Heatmap showing Spearman correlations between all measured variables for the OA isolates
445 including Treg and Th17 cell induction, *Trichuris* egg hatching, and production of SCFAs, BAs,
446 H_2S, and enzymes. Variables with insufficient data points to complete the correlation analysis
447 were removed from the heatmap.

448

449 **Figure S4. dbRDA analysis to determine effect size of bacterial enzyme production on**
450 **lymphocyte differentiation induced by the OA isolates**
451 (A) Enzyme production data used to perform the distance-based redundancy analysis (dbRDA)
452 and statistical significance of the F statistic for each variable.
453 (B) PCA biplot depicting dbRDA results for Treg and Th17 cell induction and enzyme production.
454 (C) Proportion of variance explained by 10 significant variables on the variance of Treg and Th17
455 cell induction.
456

457 **Materials and Methods**

458

459 **Gnotobiotic mice**

460 Germfree (GF) C57BL/6J were bred and maintained in flexible-film isolators at the New York
461 University Grossman School of Medicine Gnotobiotics Animal Facility. Absence of fecal bacteria
462 was confirmed monthly by evaluating the presence of 16S DNA in stool samples by qPCR as
463 previously described [83]. Minimal flora (MF) mice harboring the consortium of 15 bacteria
464 described in [52] were kept in a separate isolator. For inoculation with bacteria, GF mice were
465 housed in Bioexclusion cages (Tecniplast) with access to sterile food and water. An equal amount
466 of male and female mice 6-8 weeks of age was used for all experiments. All animal studies were
467 performed according to protocols approved by the NYU Grossman School of Medicine
468 Institutional Animal Care and Use Committee.

469

470 **Bacterial strains**

471 OA isolates were previously described [45]. The consortium of 17 Clostridia isolates (KH mix)
472 including *Clostridium aldenense* (KH28) was kindly provided by K. Honda (RIKEN Center for
473 Integrative Medical Sciences, Japan) [5]. All bacteria were cultured under anaerobic conditions
474 in an anaerobic chamber (Coy Labs). Frozen glycerol stocks (30% glycerol) of all bacteria were
475 prepared. Glycerol stocks of the OA isolates were streaked onto BRU agar plates (Anaerobe
476 Systems) and incubated anaerobically for 48 hours at 37°C. PYG broth (Anaerobe Systems)
477 inoculated with single colonies was grown at 37°C. OA1, 2, 4, 5, 6, 8, 11, 12, 13, 14, the KH mix,
478 and KH28 were grown for 24 hours. OA3, 7, 9, and 10 required 3 days to reach similar turbidity.
479 To quantify colony forming units, we performed serial dilutions of liquid culture in sterile PBS and
480 plated on BRU agar plates. Segmented Filamentous Bacteria (SFB) were kindly provided by D.
481 Littmann (NYU Grossman School of Medicine) [69] in the form of stool from GF mice
482 monocolonized with SFB. SFB burden was confirmed in stool by qPCR as described in [69].

483

484 **Enzyme activity assays**

485 OA isolates were grown anaerobically for 24 hours or 3 days, prepared as per manufacturer's
486 instructions, and inoculated onto test strips from API® ZYM, API® Rapid ID 32A, and API® 20A
487 Microbial Identification Kits (BioMerieux). Test strips were incubated at 37°C for either 4 hours or
488 24 hours and at either aerobic or anaerobic conditions depending on the manufacturer's

489 instructions, after which enzyme reactions were assessed visually based on colorimetric
490 changes.
491
492 **Quantification of SCFAs using LC-MS**
493 Bacterial cultures of OA isolates were spun down at 14,000g for 5 minutes at 4°C and supernatant
494 was collected and stored at -80°C. Cecal contents were harvested from GF mice, MF mice, or
495 mice monocolonized with OA2 and stored at -80°C. For the measurement of SCFAs in bacterial
496 liquid culture, a 10 µL aliquot of the culture was mixed with 190 µL of short-chain fatty acids
497 (SCFAs) derivatization solution (1 mM 2,2′-dipyridyl disulfide, 1 mM triphenylphosphine, and 1
498 mM 2-hydrazinoquinoline dissolved in acetonitrile). For the measurement of SCFAs in cecal
499 contents, ~10mg of cecal sample was resuspended in 50 µL of 50% MeOH (in H2O) and vortexed
500 for 10 min (some beads were added to disperse the cecal material). Then the mixture was spun
501 down, and 10 µL of supernatant was mixed with 190 µL SCFAs derivatization solution.
502
503 For both bacterial liquid culture and cecal content samples, the resulting mixtures were vortexed
504 and incubated at 60 °C for 1 hr. The mixture was centrifuged at 21000 x g for 20 min, and the
505 supernatant was analyzed using an Agilent 1290 LC system coupled to an Agilent 6530
506 quadrupole time-of-flight (QTOF) mass spectrometer with a 130Å, 1.7 µm, 2.1 mm × 100 mm
507 ACQUITY UPLC BEH C18 column (Waters). We used the following solvent system: A: H2O with
508 0.1% formic acid; B: Methanol with 0.1% formic acid. 1 µL of each sample was injected, and the
509 flow rate was 0.35 mL/min with a column temperature of 40 °C. The gradient for HPLC-MS
510 analysis was: 0-6.0 min, 99.5%-70.0% A; 6.0-9.0 min, 70.0%-2.0% A; 9.0-9.4 min, 2.0% A; 9.4-
511 9.6min, 2.0%-99.5% A. Peaks were assigned by comparison with authentic standards.
512
513 **Hydrogen sulfide production assay**
514 In a 24-well plate, 10ul of 24-hour or 3-day bacterial culture was added to 1ml of sterile PYG
515 media. Each plate was covered with a piece of lead acetate paper cut to fit the 24-well plate,
516 followed by the plate lid over the lead acetate paper. After 24 hours, photos were taken to quantify
517 darkening of the lead acetate paper using Image J.
518

519 **Quantification of Treg and Th17 cell induction**

520 Male and female germ-free C57BL/6J mice were monocolonized at 6-8 weeks of age by oral
521 gavage with ~$1x10^7$ colony forming units (CFU) of indicated bacteria. 21-28 days later, mice were
522 euthanized, and the colon and cecum were harvested. For single cell suspension, colonic and
523 cecal tissues were flushed with HBSS (Gibco), fat and Peyer's patches were removed, and the
524 tissue was cut into 5-6 pieces. Tissue bits were incubated first with 20 mL of HBSS with 2%
525 HEPES (Corning), 1% sodium pyruvate (Corning), 5mM EDTA, and 1 mM dithiothreitol (Sigma-
526 Aldrich) for 15 min at 37°C with shaking, and then with new 20 mL of HBSS with 2% HEPES, 1%
527 sodium pyruvate, 5mM EDTA for 10 min at 37°C with shaking. Tissue bits were washed in HBSS
528 + 5% FCS, minced, and then enzymatically digested with collagenase D (0.5 mg/mL, Roche) and
529 DNase I (0.01 mg/mL, Sigma-Aldrich) for 30-45 min at 37°C with shaking. Digested solutions
530 were passed through a 70 mm cell strainer (BD) and cells were subjected to gradient
531 centrifugation using 40% Percoll (Sigma-Aldrich).

532

533 Surface and transcription factor staining was performed per manufacturer's instructions in PBS +
534 2% FBS for 20 min on ice. Zombie Aqua Fixable Viability Kit (Biolegend) was used to exclude
535 dead cells. Surface markers were stained with anti-CD45 Pacific Blue, anti-CD3 FITC and anti-
536 CD4 APC-Cy7 from Biolegend. For intracellular staining of transcription factors, cells were
537 permeabilized with the eBioscience Foxp3/Transcription Factor Staining Buffer Set (Thermo
538 Fisher Scientific) at room temperature for 30 min, and then stained with anti-Foxp3 APC and anti-
539 Rorγt PE from Invitrogen, and anti-Helios PE-Cy7 from Biolegend. Samples were acquired on the
540 CytoFLEX analyzer (Beckman Coulter) and analyzed using FlowJo 10.8.1.

541

542 **Quantification of bile acids in stool samples**

543 10-15mg of stool was homogenized in cold 100% ethanol at a final concentration of 10mg/ml
544 using Zirconia/Silica 1.0mm beads. Homogenates were spun down at 21,000g for 3 minutes at
545 4°C and 450ul of the supernatant was transferred to a clean 1.5ml tube. The sample was then
546 dried down in a speedvac before reconstituting in ultrapure water. Bile acid concentration in each
547 sample was quantified using the Bile Acid Assay Kit (Sigma #MAK309) following the
548 manufacturer's instructions, and the SpectraMax M3 Multi-Mode Microplate Reader with SoftMax
549 Pro 6.5.1. software.

550

551 **Distance-based redundancy analysis (dbRDA)**

552 Enzyme production levels were normalized, and one enzyme (α-mannosidase) that had zero
553 production for all isolates was removed, for further statistical analyses. Least absolute shrinkage
554 and selection operator (LASSO) regression was used as a feature selection method of enzymatic
555 production. Enzymes that contributed significantly to prediction of Treg and Th17 induction and
556 enzymes that had significant Spearman correlation coefficients were chosen as explanatory
557 variables for dbRDA. Both analyses were conducted using R version 4.2.2.

558

559 **Statistical analysis**

560 For *in vitro* and *in vivo* experiments, the number of repeats per group is annotated in
561 corresponding figure legends. Significance for all experiments was assessed using GraphPad
562 Prism software. Specific tests are annotated in corresponding figure legends. P values correlate
563 with symbols: ns or no symbol = not significant, *$p < 0.05$, **$p < 0.01$, ***$p < 0.001$, ****$p < 0.0001$.

564 **References**

565

566 1. Turnbaugh, P.J., et al., *The human microbiome project.* Nature, 2007. **449**(7164):
567 p. 804-10.

568 2. Donaldson, G.P., S.M. Lee, and S.K. Mazmanian, Gut biogeography of the
569 bacterial microbiota. Nat Rev Microbiol, 2016. 14(1): p. 20-32.

570 3. Macpherson, A.J. and N.L. Harris, Interactions between commensal intestinal
571 bacteria and the immune system. Nat Rev Immunol, 2004. 4(6): p. 478-85.

572 4. Ruff, W.E., T.M. Greiling, and M.A. Kriegel, *Host–microbiota interactions in*
573 *immune-mediated diseases.* Nature Reviews Microbiology, 2020. **18**(9): p. 521-
574 538.

575 5. Atarashi, K., et al., Treg induction by a rationally selected mixture of Clostridia
576 strains from the human microbiota. Nature, 2013. **500**(7461): p. 232-6.

577 6. Narushima, S., et al., Characterization of the 17 strains of regulatory T cell-
578 inducing human-derived Clostridia. Gut Microbes, 2014. **5**(3): p. 333-9.

579 7. Belkaid, Y. and T.W. Hand, *Role of the microbiota in immunity and inflammation.*
580 Cell, 2014. **157**(1): p. 121-41.

581 8. Ivanov, II and K. Honda, *Intestinal commensal microbes as immune modulators.*
582 Cell Host Microbe, 2012. **12**(4): p. 496-508.

583 9. Sun, M., et al., Microbiota metabolite short chain fatty acids, GPCR, and
584 inflammatory bowel diseases. J Gastroenterol, 2017. **52**(1): p. 1-8.

585 10. Clemente, J.C., et al., *The microbiome of uncontacted Amerindians.* Sci Adv,
586 2015. **1**(3).

587 11. Fragiadakis, G.K., et al., *Links between environment, diet, and the hunter-gatherer*
588 *microbiome.* Gut Microbes, 2019. **10**(2): p. 216-227.

589 12. Groussin, M., et al., Elevated rates of horizontal gene transfer in the industrialized
590 human microbiome. Cell, 2021. **184**(8): p. 2053-2067.e18.

591 13. Sonnenburg, E.D. and J.L. Sonnenburg, *The ancestral and industrialized gut*
592 *microbiota and implications for human health.* Nat Rev Microbiol, 2019. **17**(6): p.
593 383-390.

594 14. McCall, L.I., et al., *Home chemical and microbial transitions across urbanization.*
595 Nat Microbiol, 2020. **5**(1): p. 108-115.

596 15. Vangay, P., et al., *US Immigration Westernizes the Human Gut Microbiome.* Cell,
597 2018. **175**(4): p. 962-972.e10.

598 16. De Filippo, C., et al., Impact of diet in shaping gut microbiota revealed by a
599 comparative study in children from Europe and rural Africa. Proc Natl Acad Sci U
600 S A, 2010. **107**(33): p. 14691-6.

601 17. Yatsunenko, T., et al., *Human gut microbiome viewed across age and geography.*
602 Nature, 2012. **486**(7402): p. 222-7.

603 18. Jha, A.R., et al., Gut microbiome transition across a lifestyle gradient in Himalaya.
604 PLOS Biology, 2018. **16**(11): p. e2005396.

605 19. Abdill, R.J., E.M. Adamowicz, and R. Blekhman, *Public human microbiome data*
606 *are dominated by highly developed countries.* PLOS Biology, 2022. **20**(2): p.
607 e3001536.

608 20. Pasolli, E., et al., Extensive Unexplored Human Microbiome Diversity Revealed
609 by Over 150,000 Genomes from Metagenomes Spanning Age, Geography, and
610 Lifestyle. Cell, 2019. **176**(3): p. 649-662.e20.

611 21. Kupritz, J., et al., Helminth-Induced Human Gastrointestinal Dysbiosis: a
612 Systematic Review and Meta-Analysis Reveals Insights into Altered Taxon
613 Diversity and Microbial Gradient Collapse. mBio, 2021. **12**(6): p. e0289021.

614 22. Rapin, A. and N.L. Harris, *Helminth-Bacterial Interactions: Cause and*
615 *Consequence.* Trends Immunol, 2018. **39**(9): p. 724-733.

616 23. Loke, P.n. and N.L. Harris, *Networking between helminths, microbes, and*
617 *mammals.* Cell Host & Microbe, 2023. **31**(4): p. 464-471.

618 24. Zaiss, M.M. and N.L. Harris, *Interactions between the intestinal microbiome and*
619 *helminth parasites.* Parasite Immunol, 2016. **38**(1): p. 5-11.

620 25. Walusimbi, B., et al., The effects of helminth infections on the human gut
621 microbiome: a systematic review and meta-analysis. Frontiers in Microbiomes,
622 2023. **2**.

623 26. Bethony, J., et al., Soil-transmitted helminth infections: ascariasis, trichuriasis, and
624 hookworm. Lancet, 2006. **367**(9521): p. 1521-32.

625 27. WHO, *Soil-Transmitted Helminth Infections. WHO Fact Sheets*. 2020, World
626 Health Organization: Geneva, Switzerland.

627 28. Jourdan, P.M., et al., *Soil-transmitted helminth infections.* Lancet, 2018.
628 **391**(10117): p. 252-265.

629 29. Weinstock, J.V. and D.E. Elliott, *Helminths and the IBD hygiene hypothesis.*
630 Inflamm Bowel Dis, 2009. **15**(1): p. 128-33.

631 30. Bach, J.F., The hygiene hypothesis in autoimmunity: the role of pathogens and
632 commensals. Nat Rev Immunol, 2017.

633 31. Elliott, D.E. and J.V. Weinstock, Helminth-host immunological interactions:
634 prevention and control of immune-mediated diseases. Ann N Y Acad Sci, 2012.
635 **1247**: p. 83-96.

636 32. Finlay, C.M., K.P. Walsh, and K.H. Mills, Induction of regulatory cells by helminth
637 parasites: exploitation for the treatment of inflammatory diseases. Immunol Rev,
638 2014. **259**(1): p. 206-30.

639 33. McSorley, H.J. and R.M. Maizels, Helminth infections and host immune regulation.
640 Clin Microbiol Rev, 2012. 25(4): p. 585-608.

641 34. Hang, L., et al., Heligmosomoides polygyrus bakeri infection activates colonic
642 Foxp3+ T cells enhancing their capacity to prevent colitis. J Immunol, 2013.
643 191(4): p. 1927-34.

644 35. D'Elia, R., et al., Regulatory T cells: a role in the control of helminth-driven
645 intestinal pathology and worm survival. J Immunol, 2009. **182**(4): p. 2340-8.

646 36. Klementowicz, J.E., M.A. Travis, and R.K. Grencis, *Trichuris muris: a model of*
647 *gastrointestinal parasite infection.* Semin Immunopathol, 2012. **34**(6): p. 815-28.

648 37. Maizels, R.M., Regulation of immunity and allergy by helminth parasites. Allergy,
649 2020. **75**(3): p. 524-534.

650 38. Maizels, R.M., H.H. Smits, and H.J. McSorley, Modulation of Host Immunity by
651 Helminths: The Expanding Repertoire of Parasite Effector Molecules. Immunity,
652 2018. **49**(5): p. 801-818.

653 39. Loke, P. and Y.A. Lim, *Helminths and the microbiota: parts of the hygiene*
654 *hypothesis.* Parasite Immunol, 2015. **37**(6): p. 314-23.

655 40. Lawson, M.A.E., I.S. Roberts, and R.K. Grencis, *The interplay between Trichuris*
656 *and the microbiota.* Parasitology, 2021: p. 1-8.

657 41. Zaiss, M.M., et al., The Intestinal Microbiota Contributes to the Ability of Helminths
658 to Modulate Allergic Inflammation. Immunity, 2015. **43**(5): p. 998-1010.

659 42. Ramanan, D., et al., Helminth infection promotes colonization resistance via type
660 2 immunity. Science, 2016. **352**(6285): p. 608-12.

661 43. Lopetuso, L.R., et al., Commensal Clostridia: leading players in the maintenance
662 of gut homeostasis. Gut Pathogens, 2013. **5**(1): p. 23.

663 44. Atarashi, K., et al., Induction of colonic regulatory T cells by indigenous Clostridium
664 species. Science, 2011. **331**(6015): p. 337-41.

665 45. Sargsian, S., et al., Clostridia isolated from helminth-colonized humans promote
666 the life cycle of Trichuris species. Cell Rep, 2022. **41**(9): p. 111725.

667 46. Maria, R., et al., Evaluation of Antibacterial Properties of Organic Gutta-percha
668 Solvents and Synthetic Solvents Against Enterococcus faecalis. J Int Soc Prev
669 Community Dent, 2021. **11**(2): p. 179-183.

670 47. Suchomel, M., et al., Enterococcus hirae, Enterococcus faecium and
671 Enterococcus faecalis show different sensitivities to typical biocidal agents used
672 for disinfection. J Hosp Infect, 2019. **103**(4): p. 435-440.

673 48. Koh, A., et al., From Dietary Fiber to Host Physiology: Short-Chain Fatty Acids as
674 Key Bacterial Metabolites. Cell, 2016. **165**(6): p. 1332-1345.

675 49. Arpaia, N., et al., Metabolites produced by commensal bacteria promote
676 peripheral regulatory T-cell generation. Nature, 2013. **504**(7480): p. 451-5.

677 50. Furusawa, Y., et al., Commensal microbe-derived butyrate induces the
678 differentiation of colonic regulatory T cells. Nature, 2013. **504**(7480): p. 446-50.

679 51. Smith, P.M., et al., The microbial metabolites, short-chain fatty acids, regulate
680 colonic Treg cell homeostasis. Science, 2013. **341**(6145): p. 569-73.

681 52. Brugiroux, S., et al., Genome-guided design of a defined mouse microbiota that
682 confers colonization resistance against Salmonella enterica serovar Typhimurium.
683 Nat Microbiol, 2016. **2**: p. 16215.

684 53. Dallari, S., et al., Enteric viruses evoke broad host immune responses resembling
685 those elicited by the bacterial microbiome. Cell Host Microbe, 2021. **29**(6): p.
686 1014-1029.e8.

687 54. Cui, C., et al., CD4(+) T-Cell Endogenous Cystathionine γ Lyase-Hydrogen Sulfide
688 Attenuates Hypertension by Sulfhydrating Liver Kinase B1 to Promote T
689 Regulatory Cell Differentiation and Proliferation. Circulation, 2020. **142**(18): p.
690 1752-1769.

691 55. Yang, R., et al., Hydrogen Sulfide Promotes Tet1- and Tet2-Mediated Foxp3
692 Demethylation to Drive Regulatory T Cell Differentiation and Maintain Immune
693 Homeostasis. Immunity, 2015. **43**(2): p. 251-63.

694 56. Braccia, D.J., et al., The Capacity to Produce Hydrogen Sulfide (H2S) via Cysteine
695 Degradation Is Ubiquitous in the Human Gut Microbiome. Frontiers in
696 Microbiology, 2021. **12**.

697 57. Fiorucci, S., et al., Inhibition of hydrogen sulfide generation contributes to gastric
698 injury caused by anti-inflammatory nonsteroidal drugs. Gastroenterology, 2005.
699 **129**(4): p. 1210-24.

700 58. Rahman, M.A., et al., Hydrogen sulfide dysregulates the immune response by
701 suppressing central carbon metabolism to promote tuberculosis. Proc Natl Acad
702 Sci U S A, 2020. **117**(12): p. 6663-6674.

703 59. Fiorucci, S., et al., Enhanced activity of a hydrogen sulphide-releasing derivative
704 of mesalamine (ATB-429) in a mouse model of colitis. Br J Pharmacol, 2007.
705 **150**(8): p. 996-1002.

706 60. Tanoue, T., K. Atarashi, and K. Honda, *Development and maintenance of*
707 *intestinal regulatory T cells.* Nat Rev Immunol, 2016. **16**(5): p. 295-309.

708 61. Sefik, E., et al., Individual intestinal symbionts induce a distinct population of
709 RORgamma(+) regulatory T cells. Science, 2015. **349**(6251): p. 993-7.

710 62. Ohnmacht, C., et al., *The microbiota regulates type 2 immunity through RORgt+*
711 *T cells.* Science, 2015. **349**(6251): p. 989-993.

712 63. Yang, B.H., et al., Foxp3(+) T cells expressing RORgammat represent a stable
713 regulatory T-cell effector lineage with enhanced suppressive capacity during
714 intestinal inflammation. Mucosal Immunol, 2016. **9**(2): p. 444-57.

715 64. Kanamori, M., et al., Induced Regulatory T Cells: Their Development, Stability,
716 and Applications. Trends Immunol, 2016. **37**(11): p. 803-811.

717 65. Bilate, A.M. and J.J. Lafaille, *Induced CD4+Foxp3+ regulatory T cells in immune*
718 *tolerance.* Annu Rev Immunol, 2012. **30**: p. 733-58.

719 66. Geva-Zatorsky, N., et al., *Mining the Human Gut Microbiota for*
720 *Immunomodulatory Organisms.* Cell, 2017. **168**(5): p. 928-943 e11.

721 67. Lathrop, S.K., et al., Peripheral education of the immune system by colonic
722 commensal microbiota. Nature, 2011. **478**(7368): p. 250-4.

723 68. Round, J.L. and S.K. Mazmanian, Inducible Foxp3+ regulatory T-cell development
724 by a commensal bacterium of the intestinal microbiota. Proc Natl Acad Sci U S A,
725 2010. **107**(27): p. 12204-9.

726 69. Ivanov, II, et al., Induction of intestinal Th17 cells by segmented filamentous
727 bacteria. Cell, 2009. **139**(3): p. 485-98.

728 70. Hirahara, K. and T. Nakayama, *CD4+ T-cell subsets in inflammatory diseases:*
729 *beyond the Th1/Th2 paradigm.* International immunology, 2016. **28**(4): p. 163-171.

730 71. Honda, K. and D.R. Littman, *The microbiota in adaptive immune homeostasis and*
731 *disease.* Nature, 2016. **535**(7610): p. 75-84.

732 72. Hang, S., et al., Bile acid metabolites control TH17 and Treg cell differentiation.
733 Nature, 2019. **576**(7785): p. 143-148.

734 73. Li, W., et al., A bacterial bile acid metabolite modulates T(reg) activity through the
735 nuclear hormone receptor NR4A1. Cell Host Microbe, 2021. **29**(9): p. 1366-
736 1377.e9.

737 74. Paik, D., et al., Human gut bacteria produce TH17-modulating bile acid
738 metabolites. Nature, 2022. **603**(7903): p. 907-912.

739 75. Song, X., et al., Microbial bile acid metabolites modulate gut RORγ+ regulatory T
740 cell homeostasis. Nature, 2020. **577**(7790): p. 410-415.

741 76. Zhou, D., et al., Chymotrypsin both directly modulates bacterial growth and asserts
742 ampicillin degradation-mediated protective effect on bacteria. Annals of
743 Microbiology, 2013. **63**(2): p. 623-631.

744 77. Miyoshi, S.-I., Extracellular proteolytic enzymes produced by human pathogenic
745 vibrio species. Frontiers in Microbiology, 2013. **4**.

746 78. Hurley, L.C. and R.I. Sommerville, *Reversible inhibition of hatching of infective*
747 *eggs of Ascaris suum (Nematoda).* International Journal for Parasitology, 1982.
748 **12**(5): p. 463-465.

749 79. Sonowal, R., et al., Hydrolysis of aromatic β-glucosides by non-pathogenic
750 bacteria confers a chemical weapon against predators. Proceedings. Biological
751 sciences, 2013. **280**(1762): p. 20130721-20130721.

752 80. Dziekońska-Rynko, J. and J. Rokicki, Activity of selected hydrolases in excretion-
753 secretion products and extracts of adult Contracaecum rudolphii. Wiad Parazytol,
754 2005. **51**(3): p. 227-31.

755 81. Larabi, A.B., H.L.P. Masson, and A.J. Bäumler, *Bile acids as modulators of gut*
756 *microbiota composition and function.* Gut Microbes, 2023. **15**(1): p. 2172671.

757 82. Urrutia, A., et al., Bacterially produced metabolites protect C. elegans neurons
758 from degeneration. PLoS Biol, 2020. **18**(3): p. e3000638.

759 83. Kernbauer, E., Y. Ding, and K. Cadwell, *An enteric virus can replace the beneficial*
760 *function of commensal bacteria.* Nature, 2014. **516**(7529): p. 94-8.

761

Figure 1.

	Family	Genus; species	*Trichuris* associated	Promotes *Trichuris* life cycle
OA12	*Enterococcaceae*	*Enterococcus hirae*	Yes	No
OA7	*Erysipelotrichaceae*	*Holdemania massiliensis*	No	
OA4	*Coprobacillaceae* *	*Clostridium innocuum*	No	No
OA5	*Coprobacillaceae* *	*Clostridium innocuum*	No	
OA14	*Clostridiaceae*	*Clostridium perfringens*	No	No
OA8	*Peptostreptococcaceae*	*Paeniclostridium sordellii* **	Yes	Yes
OA6	*Peptostreptococcaceae*	*Romboutsia hominis*	Yes	Yes
OA2	*Peptostreptococcaceae*	*Romboutsia hominis*	Yes	Yes
OA9	*Oscillospiraceae*	*Lawsonibacter sp. OA9*	Yes	
OA10	*Oscillospiraceae*	*Lawsonibacter asaccharolyticus*	No	
OA3	*Oscillospiraceae* *	*Ruminococcus pangsunibacterium (sp. OA3)*	No	
OA1	*Lachnospiraceae*	*Muricomes sp. OA1*	No	
OA13	*Lachnospiraceae*	*Enterocloster sp. OA13*	N.D.	
OA11	*Lachnospiraceae*	*Enterocloster sp. OA11*	N.D.	

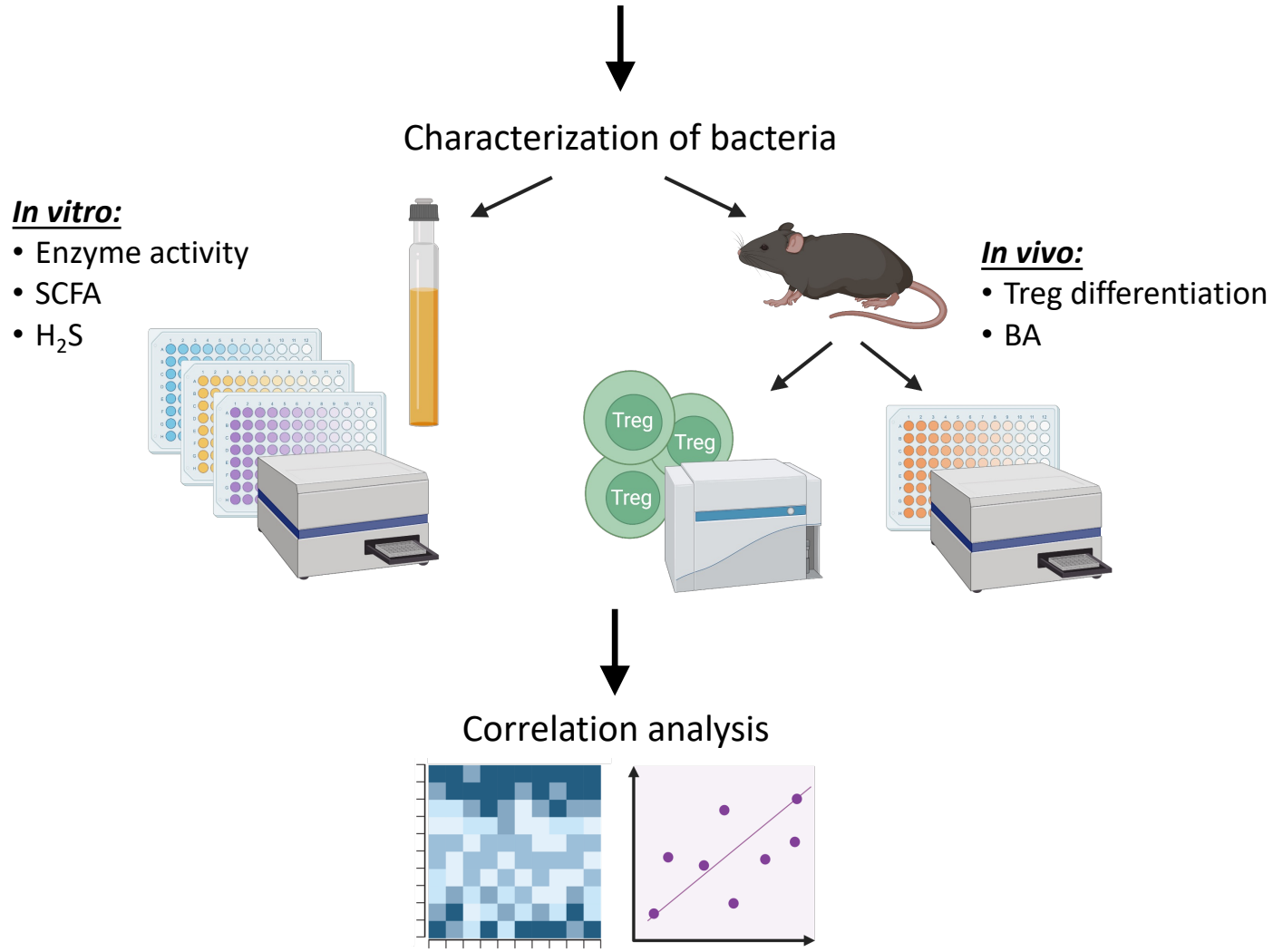

Figure 2.

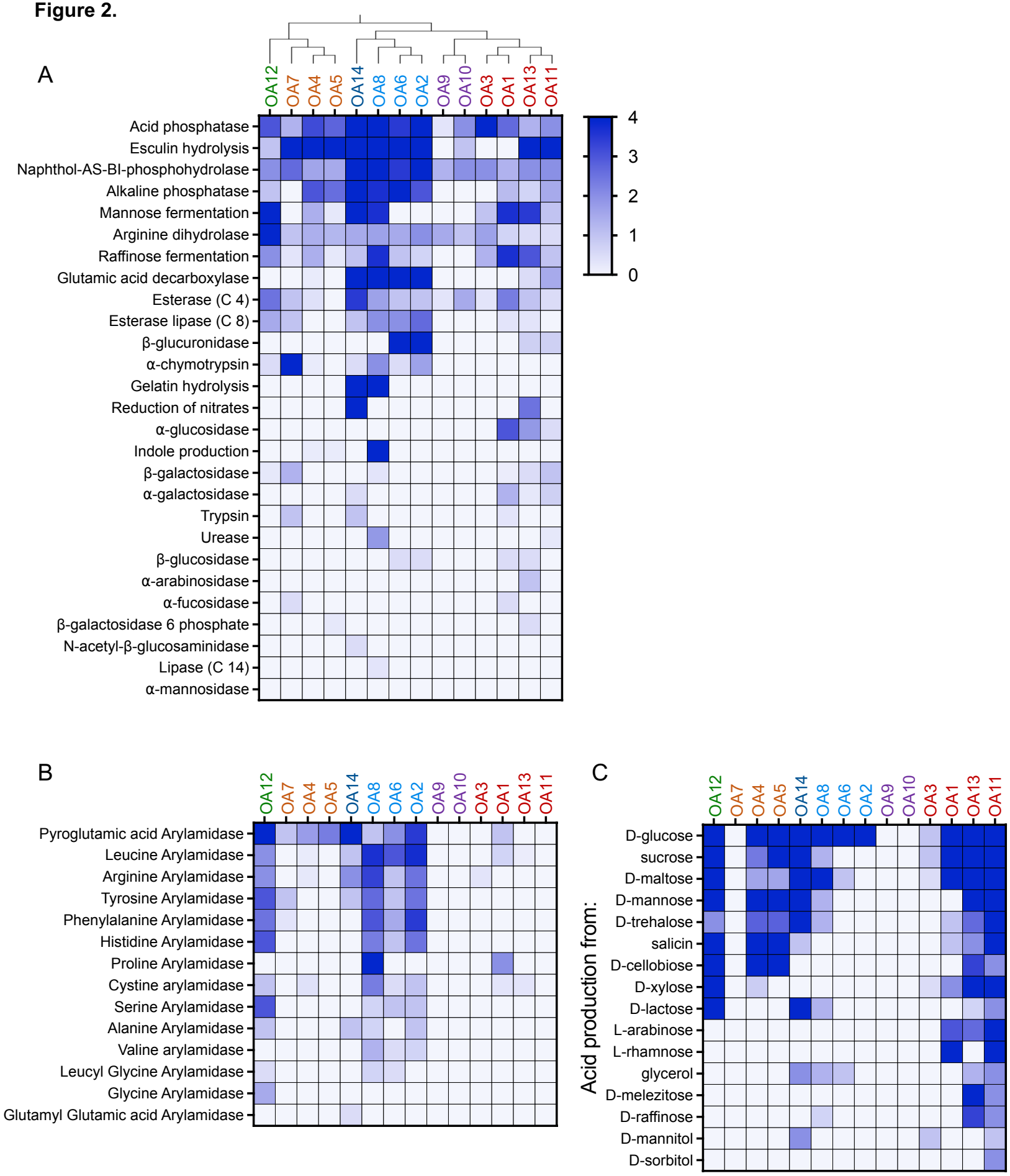
A
OA12
OA7
OA4
OA5
OA14
OA8
OA6
OA2
OA9
OA10
OA3
OA1
OA13
OA11
Acid phosphatase
Esculin hydrolysis
Naphthol-AS-BI-phosphohydrolase
Alkaline phosphatase
Mannose fermentation
Arginine dihydrolase
Raffinose fermentation
Glutamic acid decarboxylase
Esterase (C 4)
Esterase lipase (C 8)
β-glucuronidase
α-chymotrypsin
Gelatin hydrolysis
Reduction of nitrates
α-glucosidase
Indole production
β-galactosidase
α-galactosidase
Trypsin
Urease
β-glucosidase
α-arabinosidase
α-fucosidase
β-galactosidase 6 phosphate
N-acetyl-β-glucosaminidase
Lipase (C 14)
α-mannosidase
4
3
2
1
0
B
Pyroglutamic acid Arylamidase
Leucine Arylamidase
Arginine Arylamidase
Tyrosine Arylamidase
Phenylalanine Arylamidase
Histidine Arylamidase
Proline Arylamidase
Cystine arylamidase
Serine Arylamidase
Alanine Arylamidase
Valine arylamidase
Leucyl Glycine Arylamidase
Glycine Arylamidase
Glutamyl Glutamic acid Arylamidase
C
Acid production from:
D-glucose
sucrose
D-maltose
D-mannose
D-trehalose
salicin
D-cellobiose
D-xylose
D-lactose
L-arabinose
L-rhamnose
glycerol
D-melezitose
D-raffinose
D-mannitol
D-sorbitol

Figure 3.

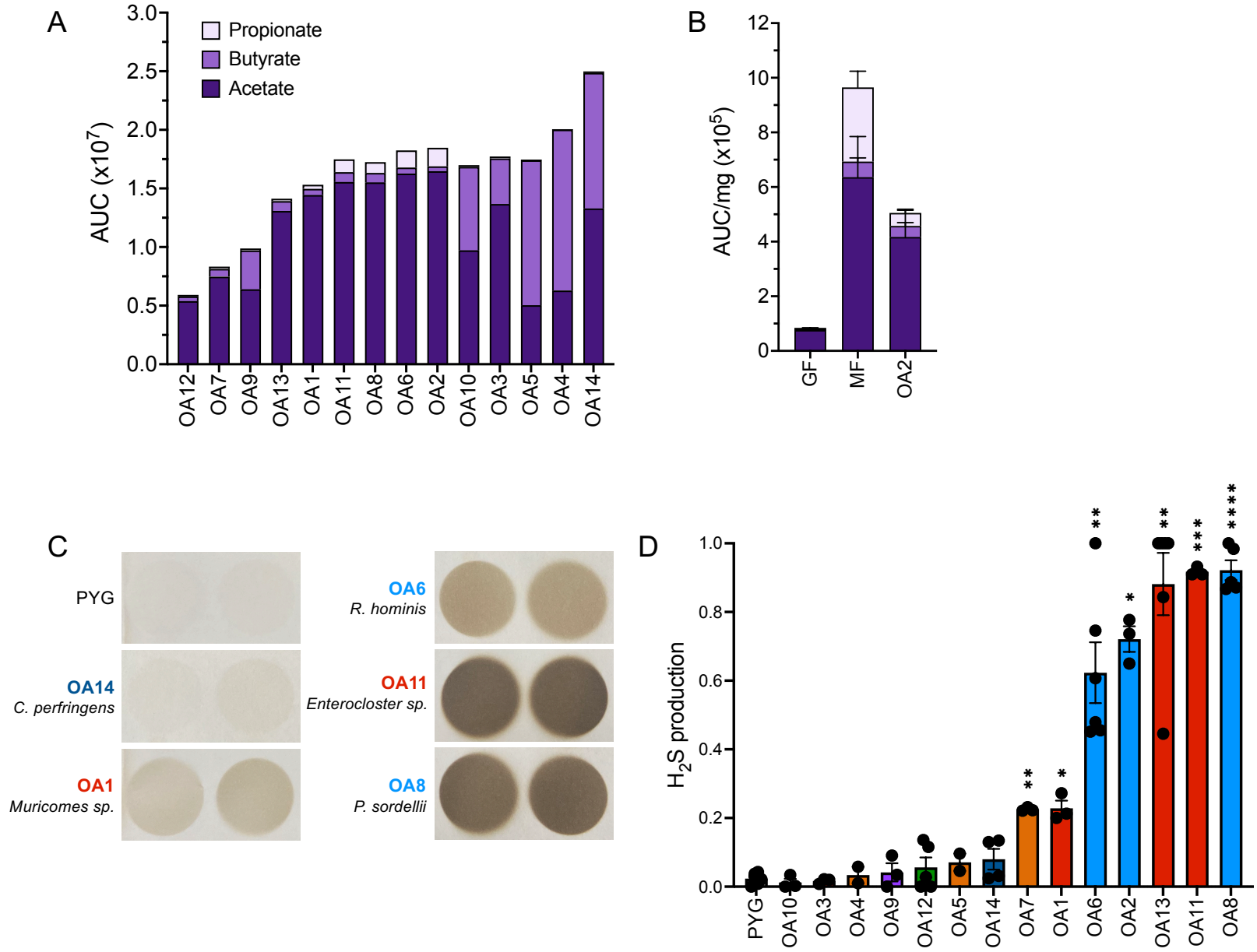
A
Propionate
Butyrate
Acetate
AUC (x10^7)
3.0
2.5
2.0
1.5
1.0
0.5
0.0
OA12
OA7
OA9
OA13
OA1
OA11
OA8
OA6
OA2
OA10
OA3
OA5
OA4
OA14
B
AUC/mg (x10^5)
12
10
8
6
4
2
0
GF
MF
OA2
C
PYG
OA14
C. perfringens
OA1
Muricomes sp.
OA6
R. hominis
OA11
Enterocloster sp.
OA8
P. sordellii
D
H2S production
1.0
0.8
0.6
0.4
0.2
0.0
PYG
OA10
OA3
OA4
OA9
OA12
OA5
OA14
OA7
OA1
OA6
OA2
OA13
OA11
OA8

Figure 4.

A

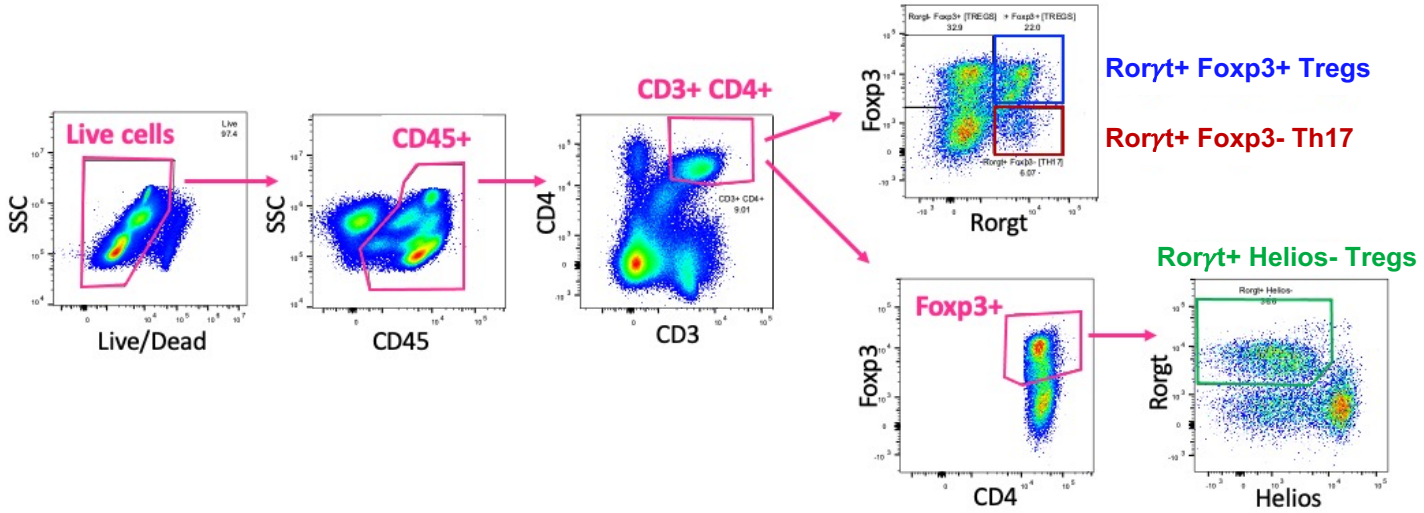
Live cells
SSC
Live/Dead
CD45+
SSC
CD45
CD3+ CD4+
CD4
CD3
Foxp3
Rorgt
Rorγt+ Foxp3+ Tregs
Rorγt+ Foxp3- Th17
Foxp3+
Foxp3
CD4
Rorγt+ Helios- Tregs
Rorgt
Helios

B

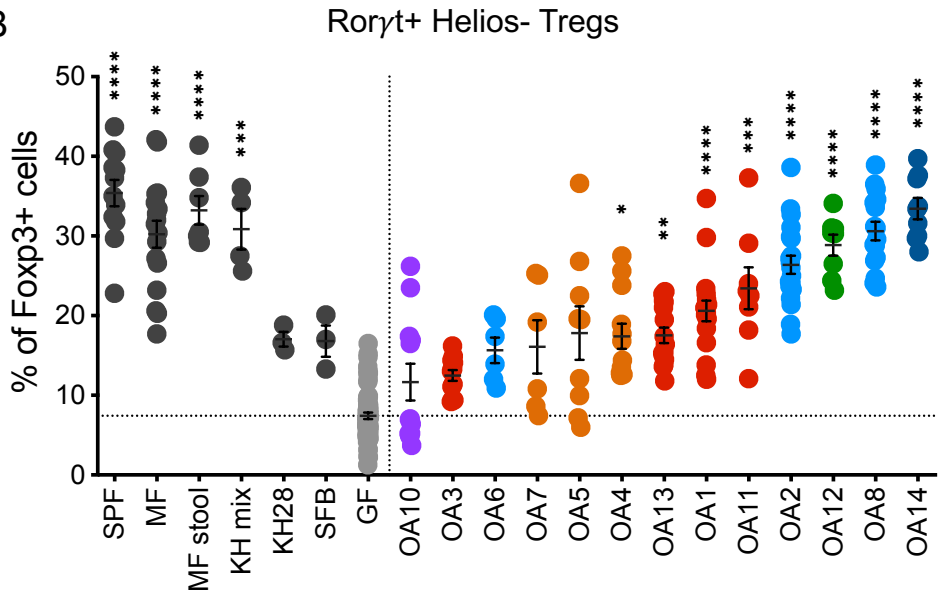
Rorγt+ Helios- Tregs
% of Foxp3+ cells
0
10
20
30
40
50
SPF
MF
MF stool
KH mix
KH28
SFB
GF
OA10
OA3
OA6
OA7
OA5
OA4
OA13
OA1
OA11
OA2
OA12
OA8
OA14

C

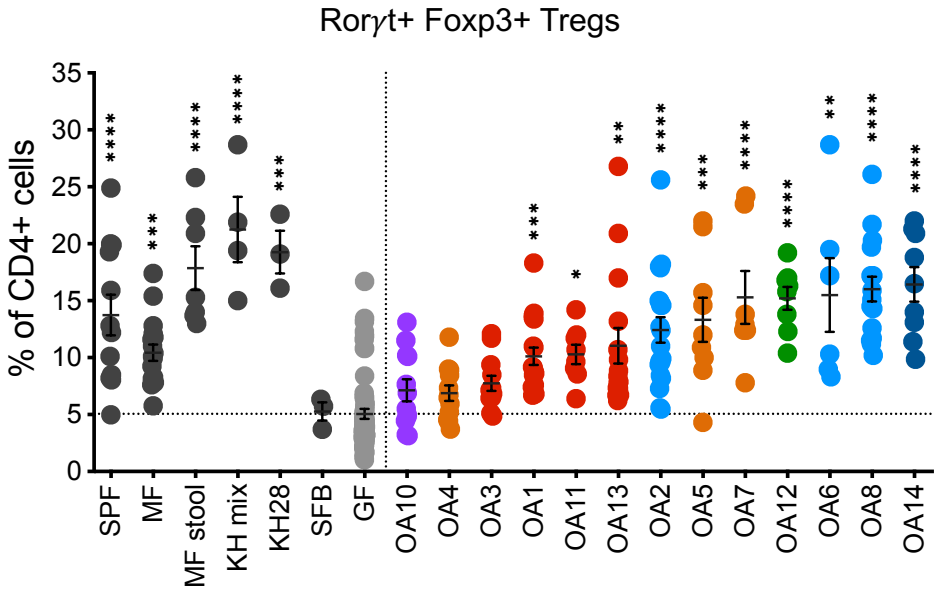
Rorγt+ Foxp3+ Tregs
% of CD4+ cells
0
5
10
15
20
25
30
35
SPF
MF
MF stool
KH mix
KH28
SFB
GF
OA10
OA4
OA3
OA1
OA11
OA13
OA2
OA5
OA7
OA12
OA6
OA8
OA14

Figure 5.

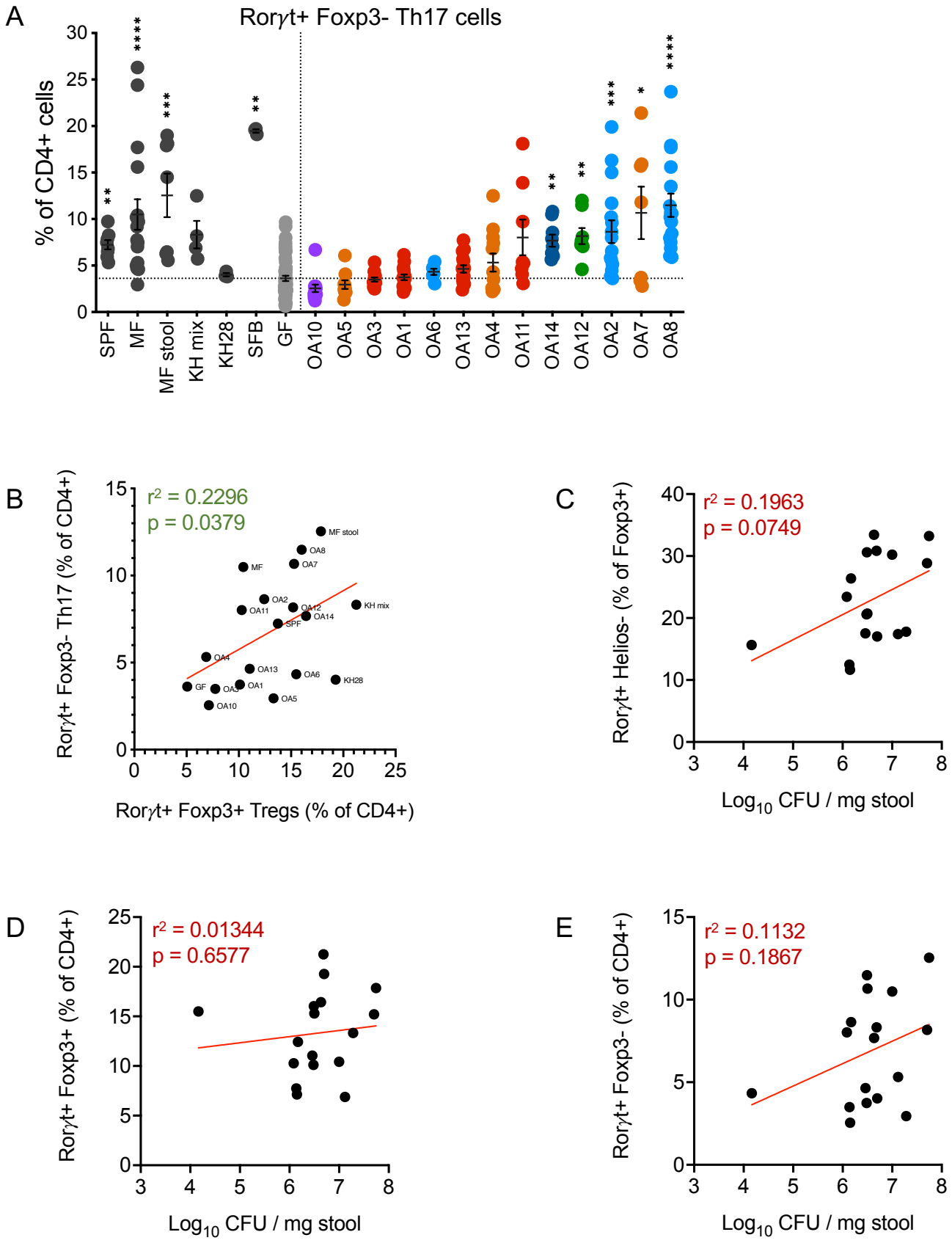
A
Rorγt+ Foxp3- Th17 cells
% of CD4+ cells
SPF
MF
MF stool
KH mix
KH28
SFB
GF
OA10
OA5
OA3
OA1
OA6
OA13
OA4
OA11
OA14
OA12
OA2
OA7
OA8
B
r² = 0.2296
p = 0.0379
Rorγt+ Foxp3- Th17 (% of CD4+)
Rorγt+ Foxp3+ Tregs (% of CD4+)
C
r² = 0.1963
p = 0.0749
Rorγt+ Helios- (% of Foxp3+)
Log10 CFU / mg stool
D
r² = 0.01344
p = 0.6577
Rorγt+ Foxp3+ (% of CD4+)
Log10 CFU / mg stool
E
r² = 0.1132
p = 0.1867
Rorγt+ Foxp3- (% of CD4+)
Log10 CFU / mg stool

Figure 6.

A

Variable A	Variable B	Spearman r	p value
Th17 cells: Rorγt+ Foxp3- (% of CD4+)	α-chymotrypsin	0.81117	0.00148
Treg cells: Rorγt+ Helios- (% of Foxp3+)	Alanine Arylamidase	0.78493	0.00210
Th17 cells: Rorγt+ Foxp3- (% of CD4+)	Tyrosine Arylamidase	0.73952	0.00579
Treg cells: Rorγt+ Foxp3+ (% of CD4+)	Tyrosine Arylamidase	0.73952	0.00579
Treg cells: Rorγt+ Foxp3+ (% of CD4+)	Esterase Lipase (C 8)	0.71527	0.00819
Treg cells: Rorγt+ Helios- (% of Foxp3+)	Acid production from D-lactose	0.69976	0.01008
Th17 cells: Rorγt+ Foxp3- (% of CD4+)	Phenylalanine Arylamidase	0.68912	0.01147
Treg cells: Rorγt+ Foxp3+ (% of CD4+)	Naphthol-AS-BI-phosphohydrolase	0.68221	0.01228
Treg cells: Rorgt+ Foxp3+ (% of CD4+)	α-chymotrypsin	0.67452	0.01431
Treg cells: Rorγt+ Helios- (% of Foxp3+)	Tyrosine Arylamidase	0.67338	0.01469
Th17 cells: Rorγt+ Foxp3- (% of CD4+)	Esterase Lipase (C 8)	0.64715	0.02003
Treg cells: Rorγt+ Foxp3+ (% of CD4+)	gelatin hydrolase	0.62678	0.02564
Treg cells: Rorγt+ Helios- (% of Foxp3+)	gelatin hydrolase	0.62678	0.02564
Th17 cells: Rorγt+ Foxp3- (% of CD4+)	Naphthol-AS-BI-phosphohydrolase	0.61399	0.02872
Th17 cells: Rorγt+ Foxp3- (% of CD4+)	Alanine Arylamidase	0.58193	0.04196
Th17 cells: Rorγt+ Foxp3- (% of CD4+)	H2S production	0.56593	0.04733
Treg cells: Rorγt+ Helios- (% of Foxp3+)	α-chymotrypsin	0.56404	0.04793

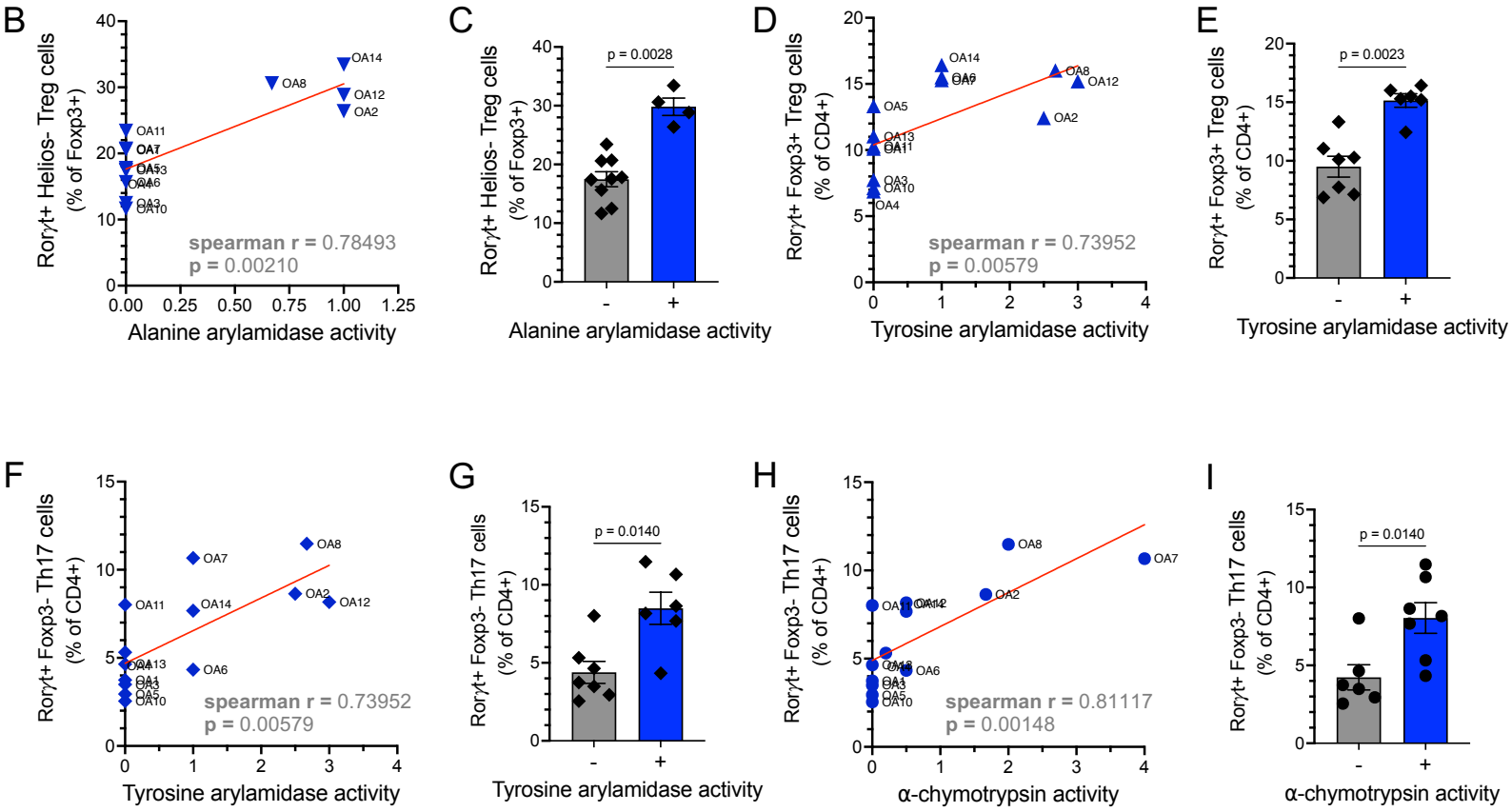

Figure 7.

A

Variable A	Variable B	Spearman r	p value
T. trichiura egg hatching	H_2S production	0.94286	0.01667
T. trichiura egg hatching	Valine Arylamidase	0.94112	0.01667
T. muris egg hatching	Valine Arylamidase	0.94112	0.01667
T. trichiura egg hatching	Acid production from salicin	-0.92582	0.03333

B

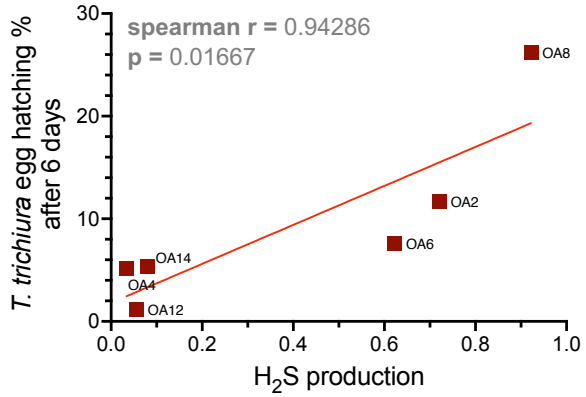

C

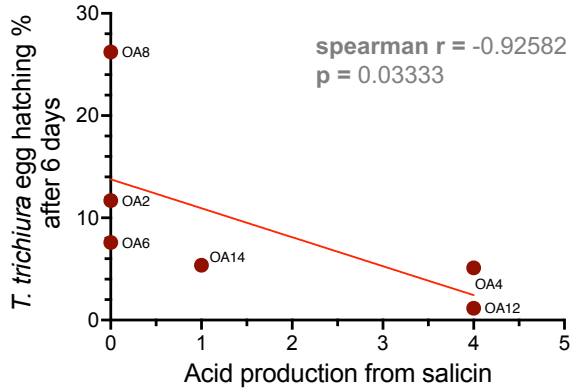

D

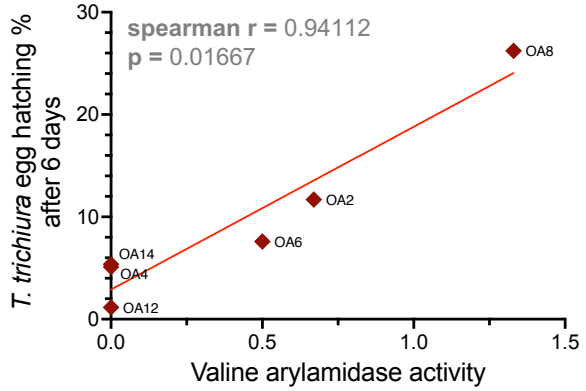

E

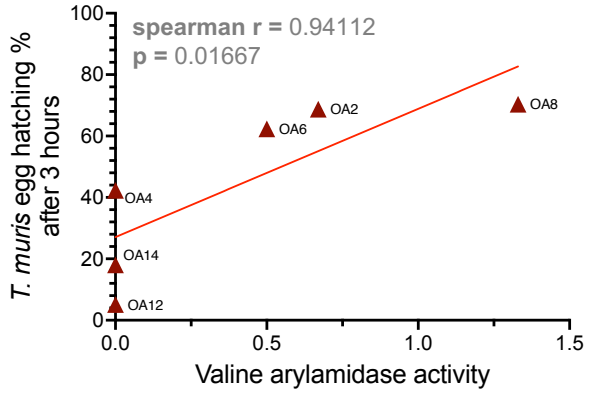

SUPPLEMENTAL FIGURES

Figure S1.

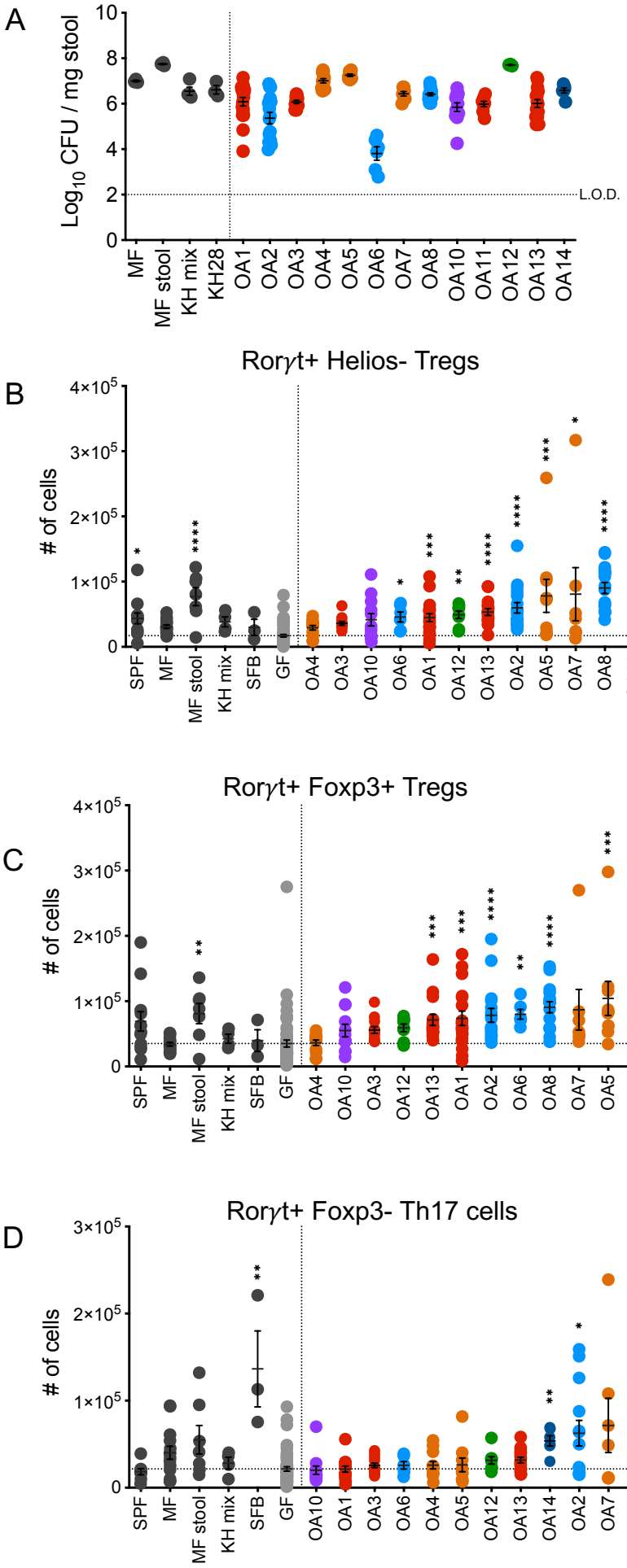

Figure S2.

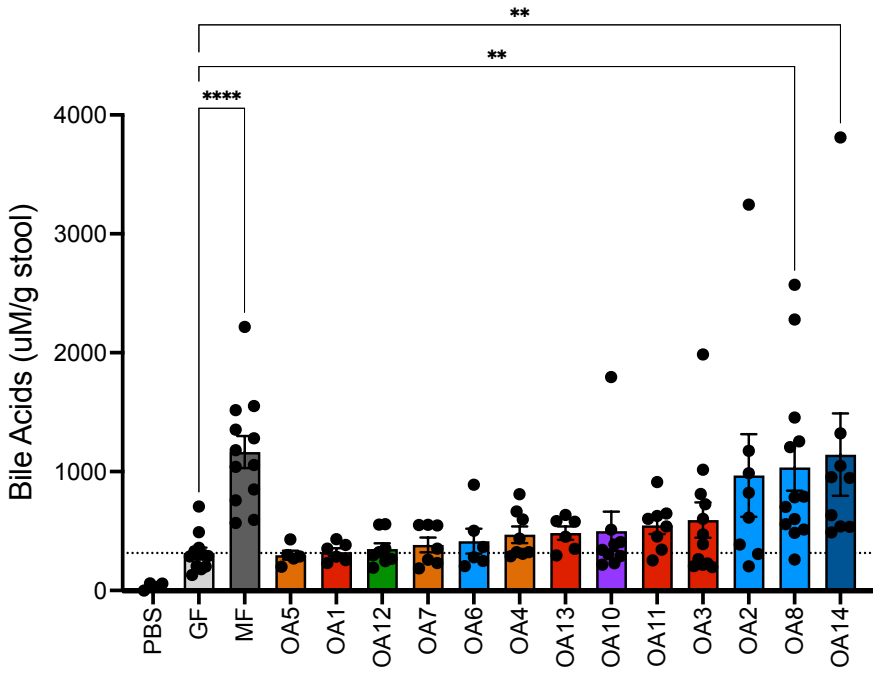
**
**
****
4000
3000
2000
1000
0
Bile Acids (uM/g stool)
PBS
GF
MF
OA5
OA1
OA12
OA7
OA6
OA4
OA13
OA10
OA11
OA3
OA2
OA8
OA14

Figure S3.

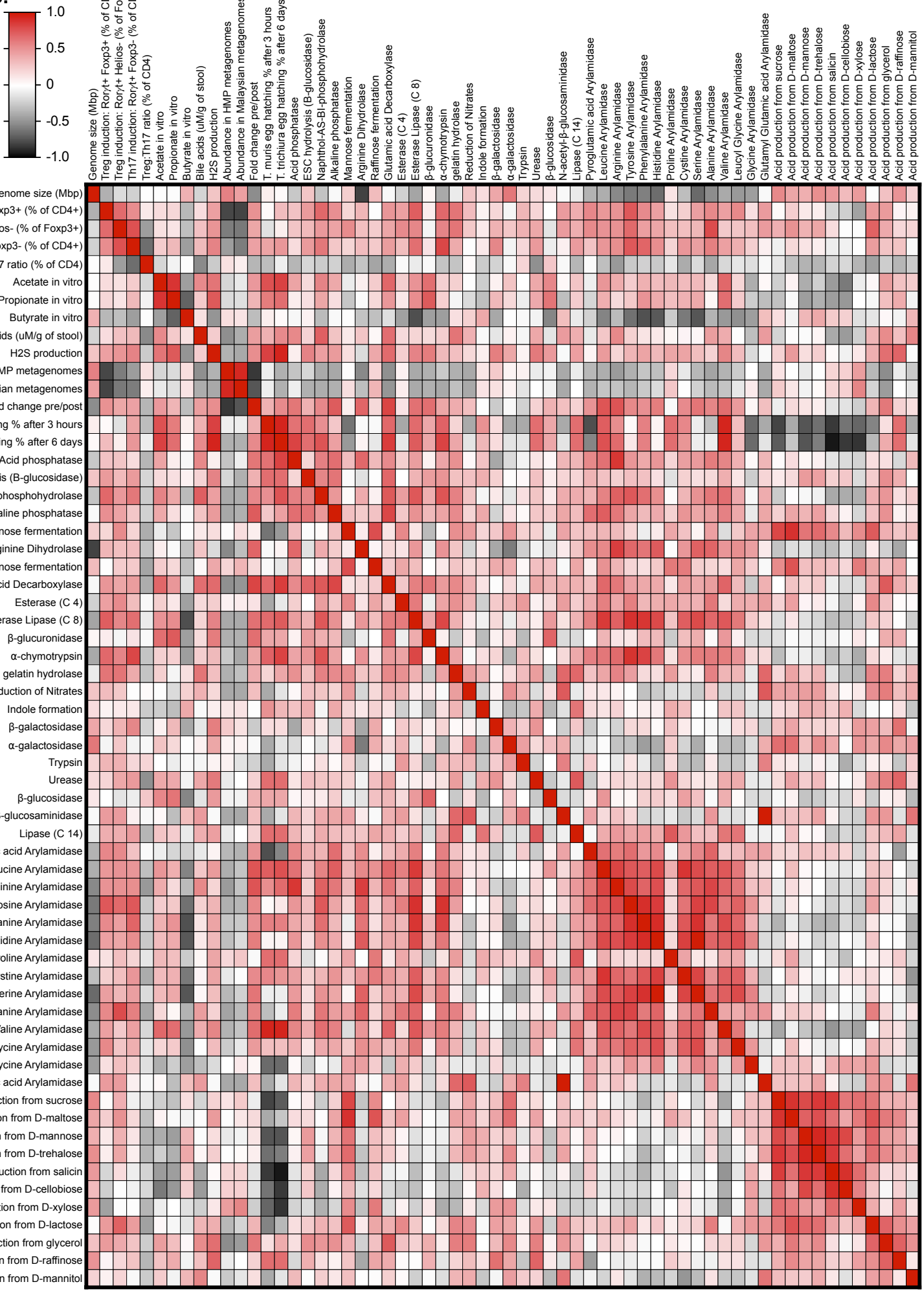
1.0
0.5
0
-0.5
-1.0
Genome size (Mbp)
Treg induction: Rorγt+ Foxp3+ (% of CD4+)
Treg induction: Rorγt+ Helios- (% of Foxp3+)
Th17 induction: Rorγt+ Foxp3- (% of CD4+)
Treg:Th17 ratio (% of CD4)
Acetate in vitro
Propionate in vitro
Butyrate in vitro
Bile acids (uM/g of stool)
H2S production
Abundance in HMP metagenomes
Abundance in Malaysian metagenomes
Fold change pre/post
T. muris egg hatching % after 3 hours
T. trichiura egg hatching % after 6 days
Acid phosphatase
ESC hydrolysis (B-glucosidase)
Naphthol-AS-BI-phosphohydrolase
Alkaline phosphatase
Mannose fermentation
Arginine Dihydrolase
Raffinose fermentation
Glutamic acid Decarboxylase
Esterase (C 4)
Esterase Lipase (C 8)
β-glucuronidase
α-chymotrypsin
gelatin hydrolase
Reduction of Nitrates
Indole formation
β-galactosidase
α-galactosidase
Trypsin
Urease
β-glucosidase
N-acetyl-β-glucosaminidase
Lipase (C 14)
Pyroglutamic acid Arylamidase
Leucine Arylamidase
Arginine Arylamidase
Tyrosine Arylamidase
Phenylalanine Arylamidase
Histidine Arylamidase
Proline Arylamidase
Cystine Arylamidase
Serine Arylamidase
Alanine Arylamidase
Valine Arylamidase
Leucyl Glycine Arylamidase
Glycine Arylamidase
Glutamyl Glutamic acid Arylamidase
Acid production from sucrose
Acid production from D-maltose
Acid production from D-mannose
Acid production from D-trehalose
Acid production from salicin
Acid production from D-cellobiose
Acid production from D-xylose
Acid production from D-lactose
Acid production from glycerol
Acid production from D-raffinose
Acid production from D-mannitol

Figure S4.

A

Explanatory variables used for dbRDA	ANOVA for each explanatory variable
Valine arylamidase	Pr(>F) = 0.003
α-chymotrypsin	Pr(>F) = 0.004
Alanine Arylamidase	Pr(>F) = 0.001
Tyrosine Arylamidase	Not significant
Esterase Lipase (C 8)	Pr(>F) = 0.028
Acid production from D-lactose	Pr(>F) = 0.002
Phenylalanine Arylamidase	Pr(>F) = 0.029
Naphthol-AS-BI-phosphohydrolase	Pr(>F) = 0.007
Gelatin hydrolase	Not significant
Acid production from salicin	Pr(>F) = 0.049
Acid production from D-trehalose	Pr(>F) = 0.045

B

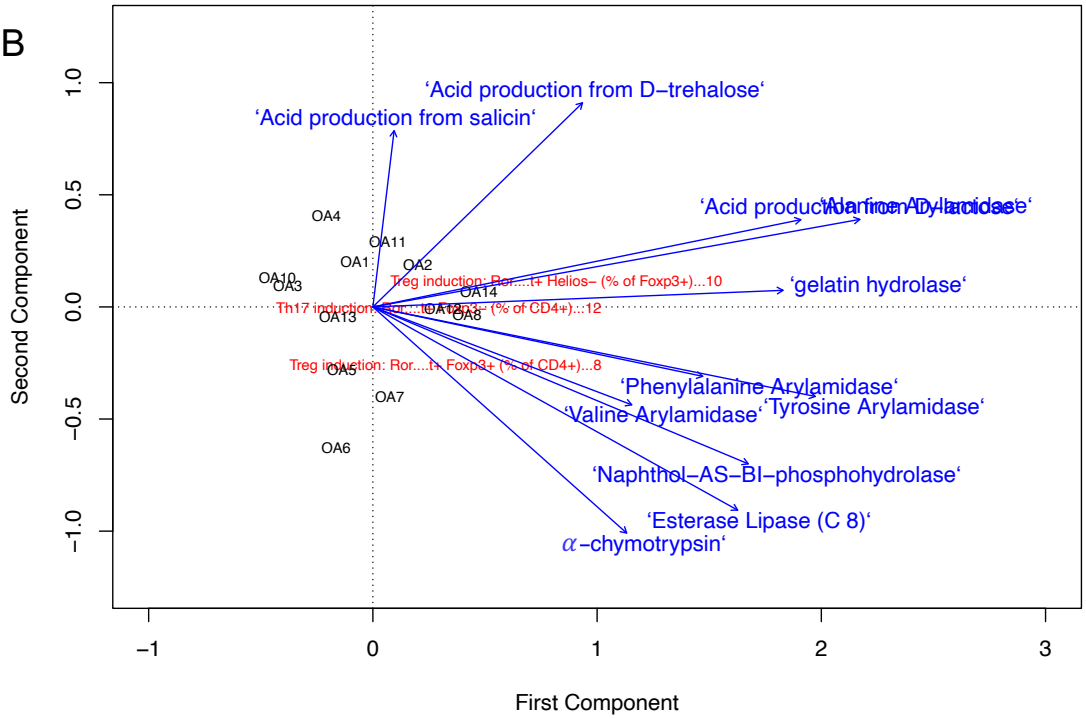

- **ANOVA for dbRDA model:** Pr(>F) = 0.009
- **ANOVA for dbRDA component 1:** Pr(>F) = 0.013 Explains 85% of the variance. Component 2 is not significant.
- **Proportion of constrained variance** > 0.99

C

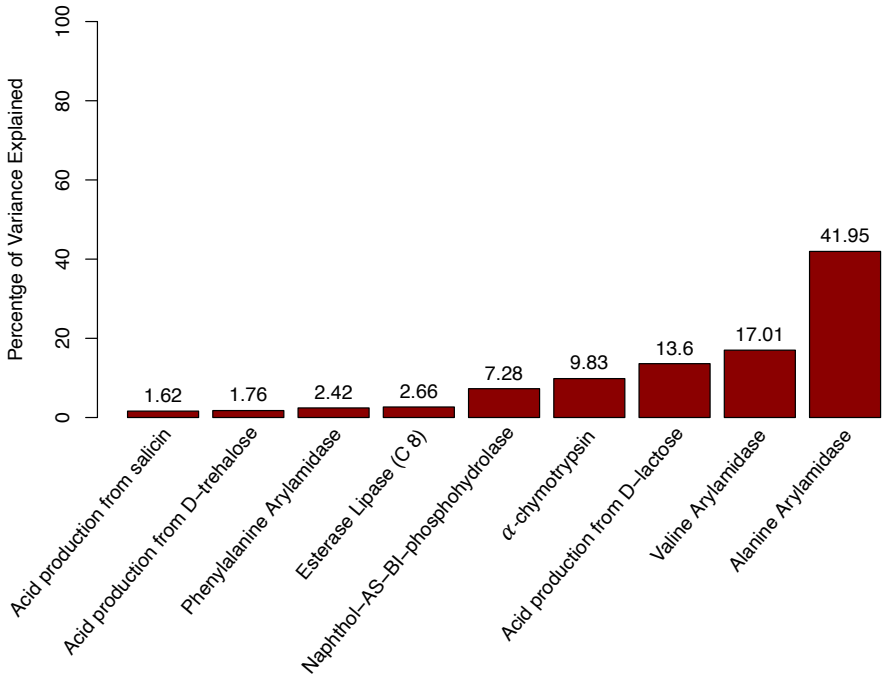

Table S1. Least absolute shrinkage and selection operator (LASSO) regression was performed to identify variables that could predict Treg and Th17 cell induction by the OA isolates. R^2 values for the model are depicted next to each cell population type, and important variables and their corresponding coefficients are below.

Treg induction: Rorγt+ Foxp3+ (% of CD4+), $R^2 > 0.3$	
Variable	Coefficient
Esterase Lipase (C 8)	1.73E-02
Treg induction: Rorγt+ Helios- (% of Foxp3+), $R^2 > 0.99$	
Variable	Coefficient
Alanine Arylamidase	3.44E-01
Alpha-Chymotrypsin	6.94E-02
Beta-galactosidase	4.02E-02
Alpha-Arabinosidase	-3.88E-02
Gelatin Hydrolase	3.27E-02
Acid production from L-rhamnose	2.97E-02
Acid production from D-trehalose	2.92E-02
Acid production from D-maltose	2.68E-02
Acid production from D-glucose	1.64E-02
Pyroglutamic Acid Arylamidase	1.33E-02
Th17 cell induction: Rorγt+ Foxp3- (% of CD4+), $R^2 > 0.97$	
Variable	Coefficient
Beta-Galactosidase	1.24E-01
Beta-Galactosidase 6 Phosphate	-5.88E-02
Arginine Arylamidase	4.77E-02
Alpha-Chymotrypsin	3.19E-02
Alanine Arylamidase	2.19E-02
Cysteine Arylamidase	1.12E-02
Acid Production from D-trehalose	1.10E-02
Acid Production from D-sorbitol	4.18E-03
ESC Hydrolysis (B-glucosidase)	3.94E-04